Supplementary Materials for

Zoonosis at the Huanan Seafood Market: A Critique

Daoyu Zhang et al.

This PDF file includes:

Supplemeary Figures
Supplementary Information

Supplementary Figures

Supp. Fig. 1. Looking West along 5th street. Male and Female toilets entrance below yellow sight at left rear of image. After WHO Mission (2021).

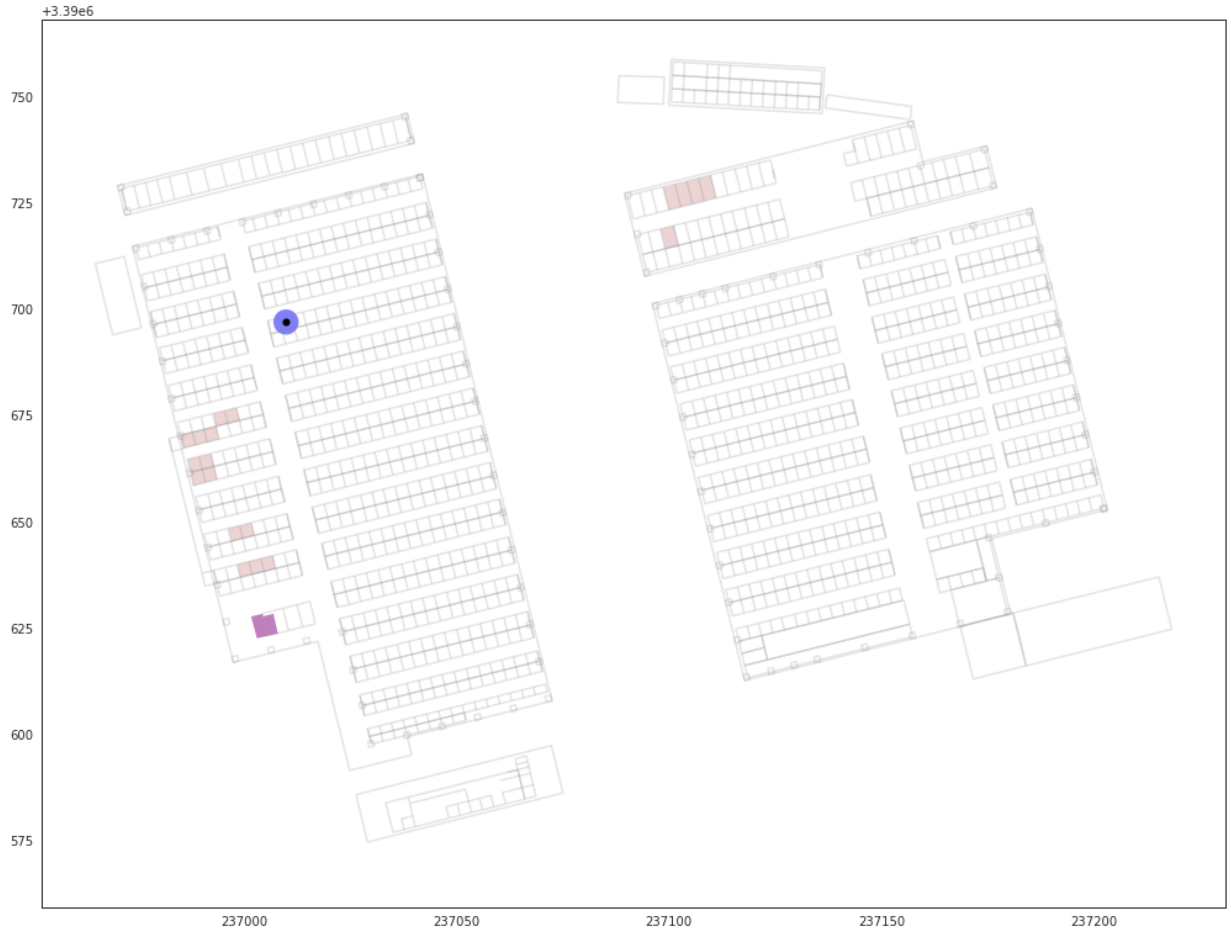

Supp. Fig. 2. COVID-19 cases at the HSM as at the 13th December 2019. A 3m buffer was drawn around cases (blue). Wild animal stalls in pink, toilets in maroon.

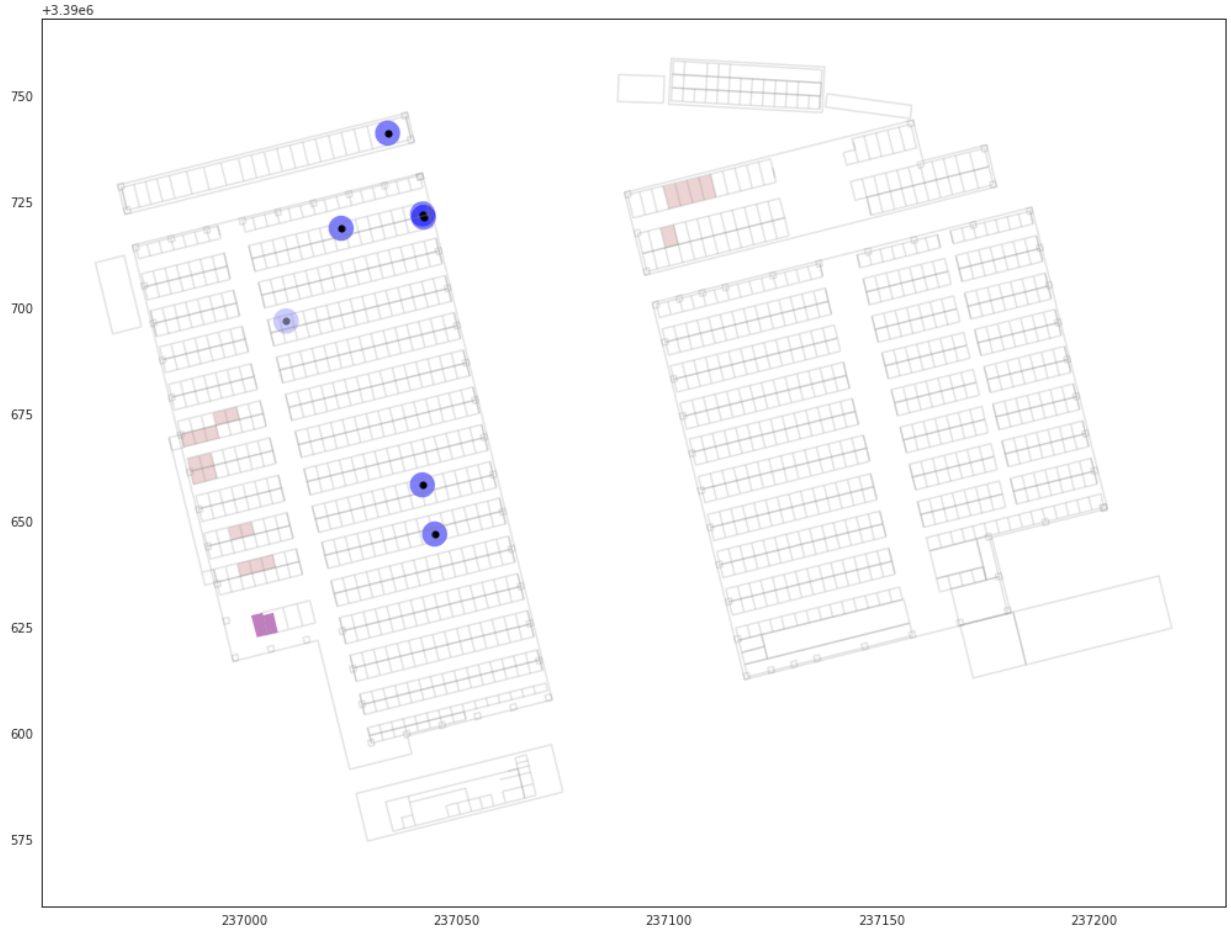

Supp. Fig. 3. COVID-19 cases at the HSM as at the 20th December 2019.A jitter of 10-50cm was randomly added/subtracted to case coordinates. A 3m buffer was drawn around new cases (blue). Cases at or earlier than 13th December shown in light blue. Wild animal stalls in pink, toilets in maroon.

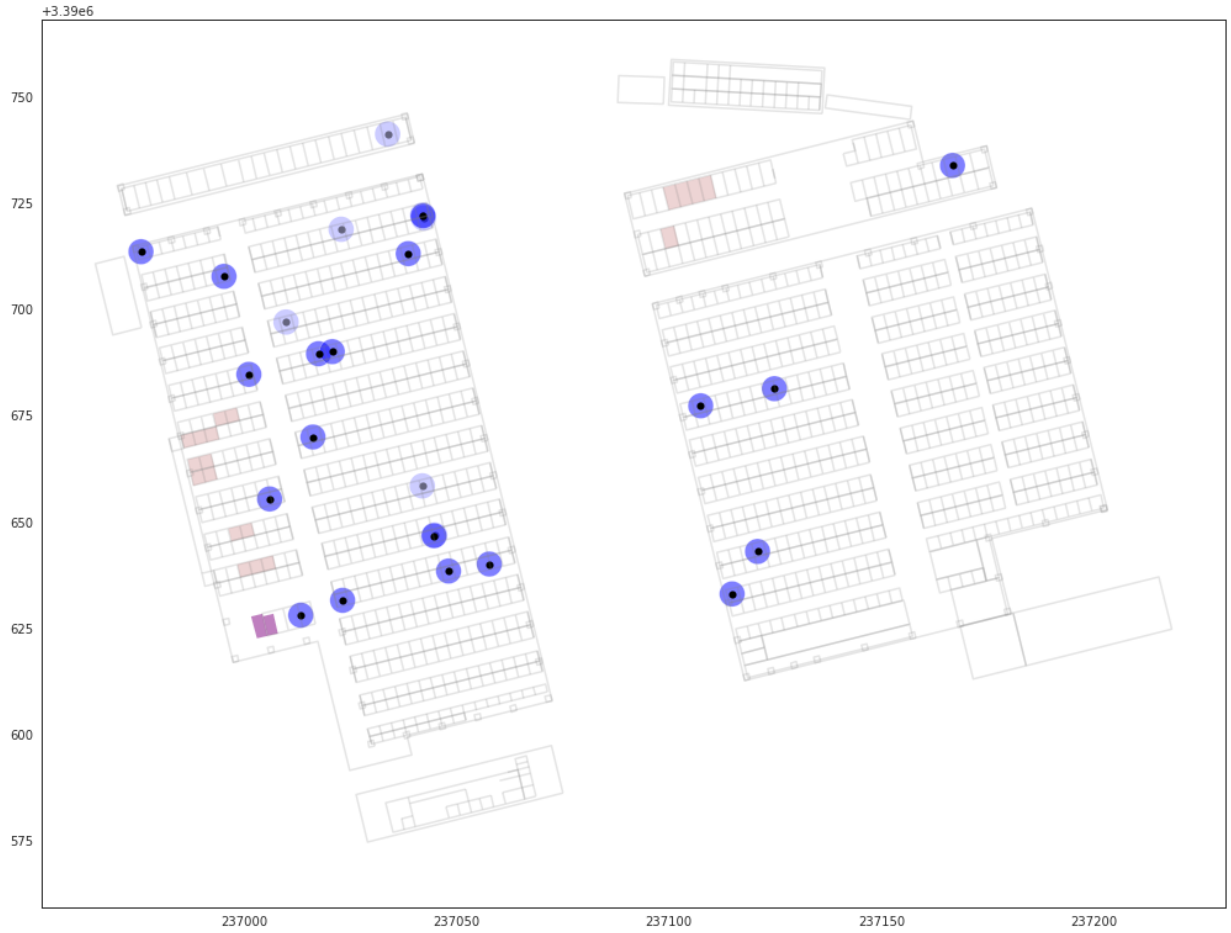

Supp. Fig. 4. COVID-19 cases at the HSM as at the 27th December 2019.A jitter of 10-50cm was randomly added/subtracted to case coordinates. A 3m buffer was drawn around new cases (blue). Cases at or earlier than 20th December shown in light blue. Wild animal stalls in pink, toilets in maroon.

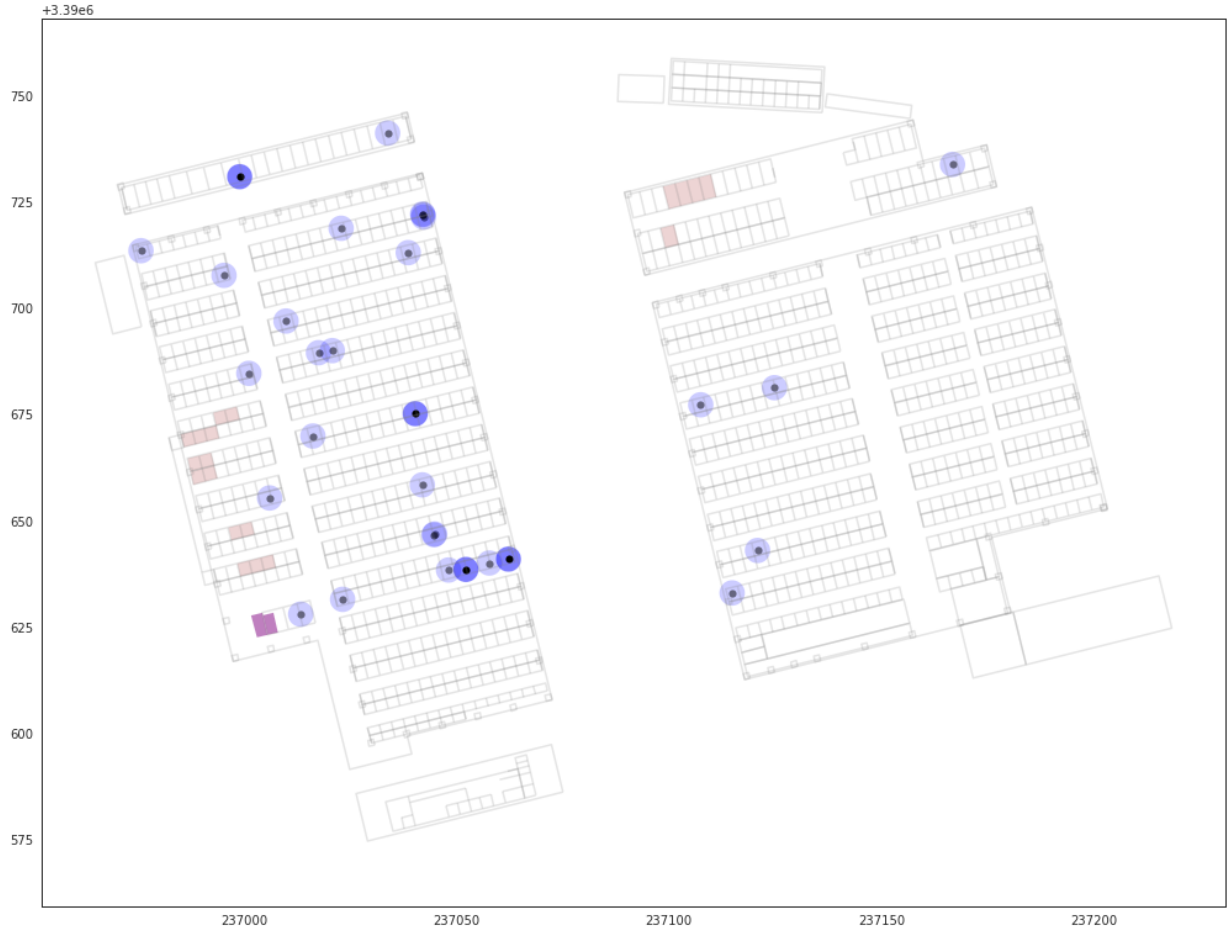

Supp. Fig. 5. COVID-19 cases at the HSM as at the 31th December 2019.A jitter of 10-50cm was randomly added/subtracted to case coordinates. A 3m buffer was drawn around new cases (blue). Cases at or earlier than 27th December shown in light blue. Wild animal stalls in pink, toilets in maroon.

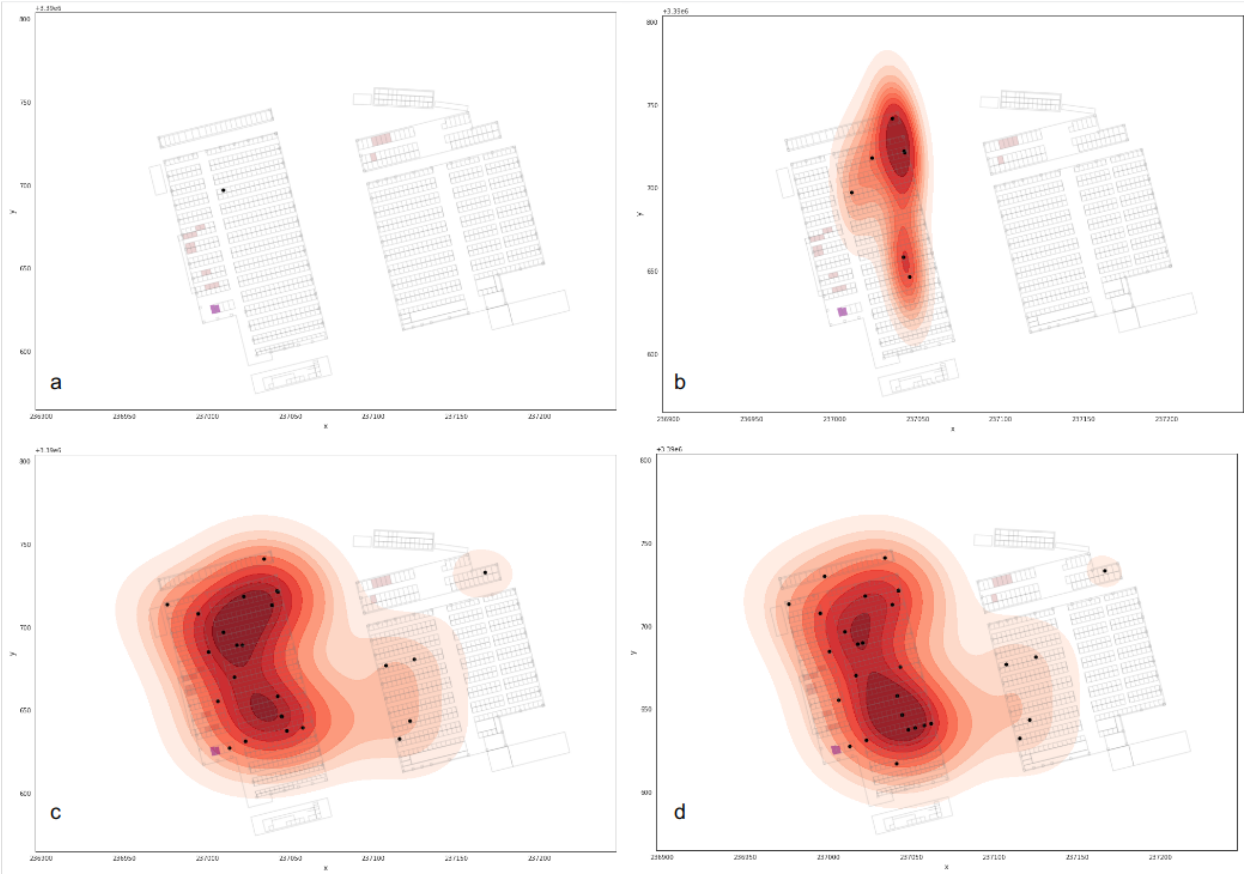

Sup. Fig. 6. COVID-19 cases KDE contour maps. a) at the HSM as at the 13th December 2019 (1 case); b) as at 20th December; c) as at 27th December; d) as at 31st December 2019. Wild animal stalls in pink, toilets in maroon, COVID-19 cases as black dots. At no stage of the outbreak at the HSM was highest case density centered on the wildlife stalls at the SW corner of the West side or the NW corner of the East side of the HSM.

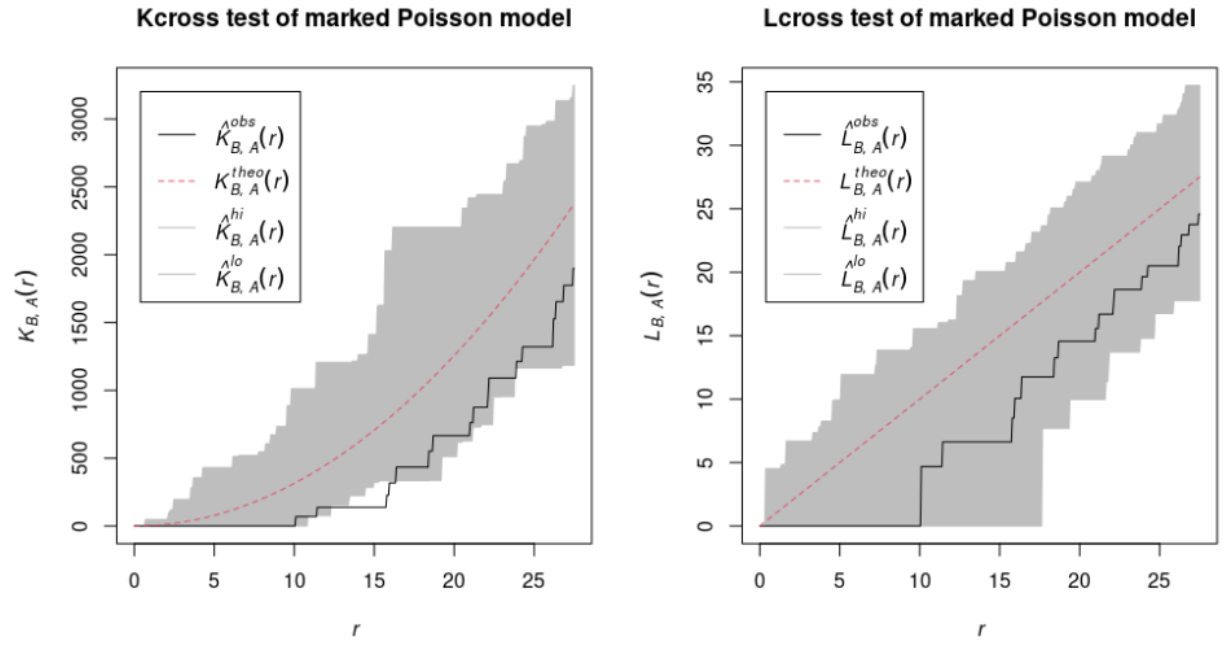

Supp. Fig. 7. Spatstas (Baddeley and Turner 2005) a) Kcross and b) Lcross functions applied to wildlife stall locations (B), superimposed with COVID-19 cases (A), in the Western section of the market only.

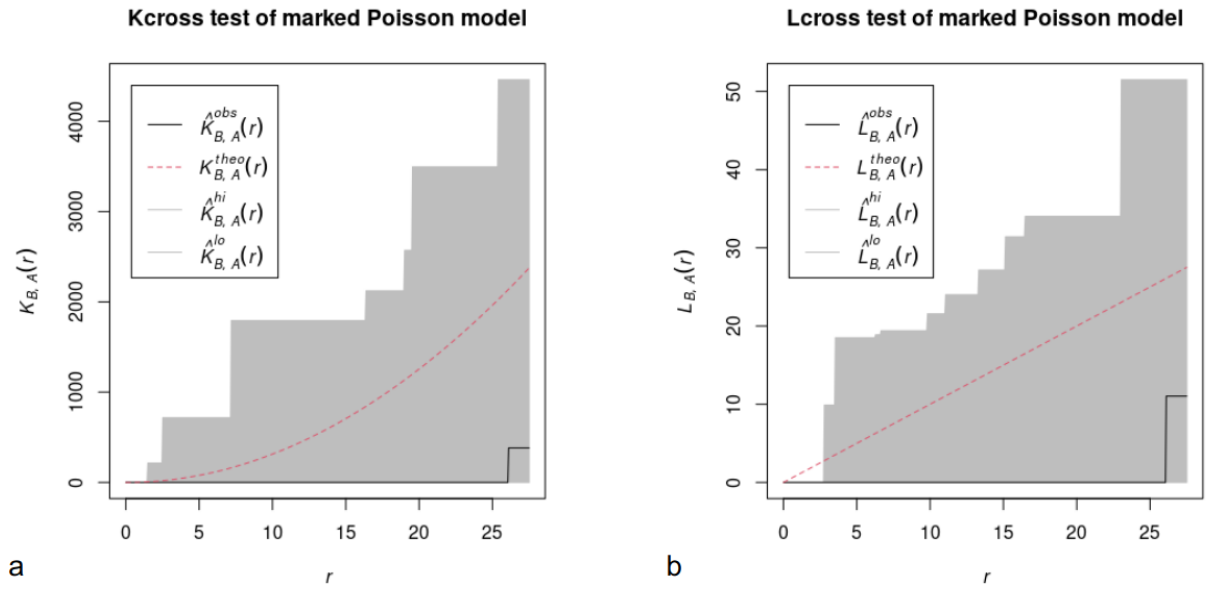

Supp. Fig. 8. Spatstats (Baddeley and Turner 2005) a) Kcross and b) Lcross functions applied to wildlife stall locations (B), superimposed with COVID-19 cases (A), as at 20 December 2019 in the Western section of the market only.

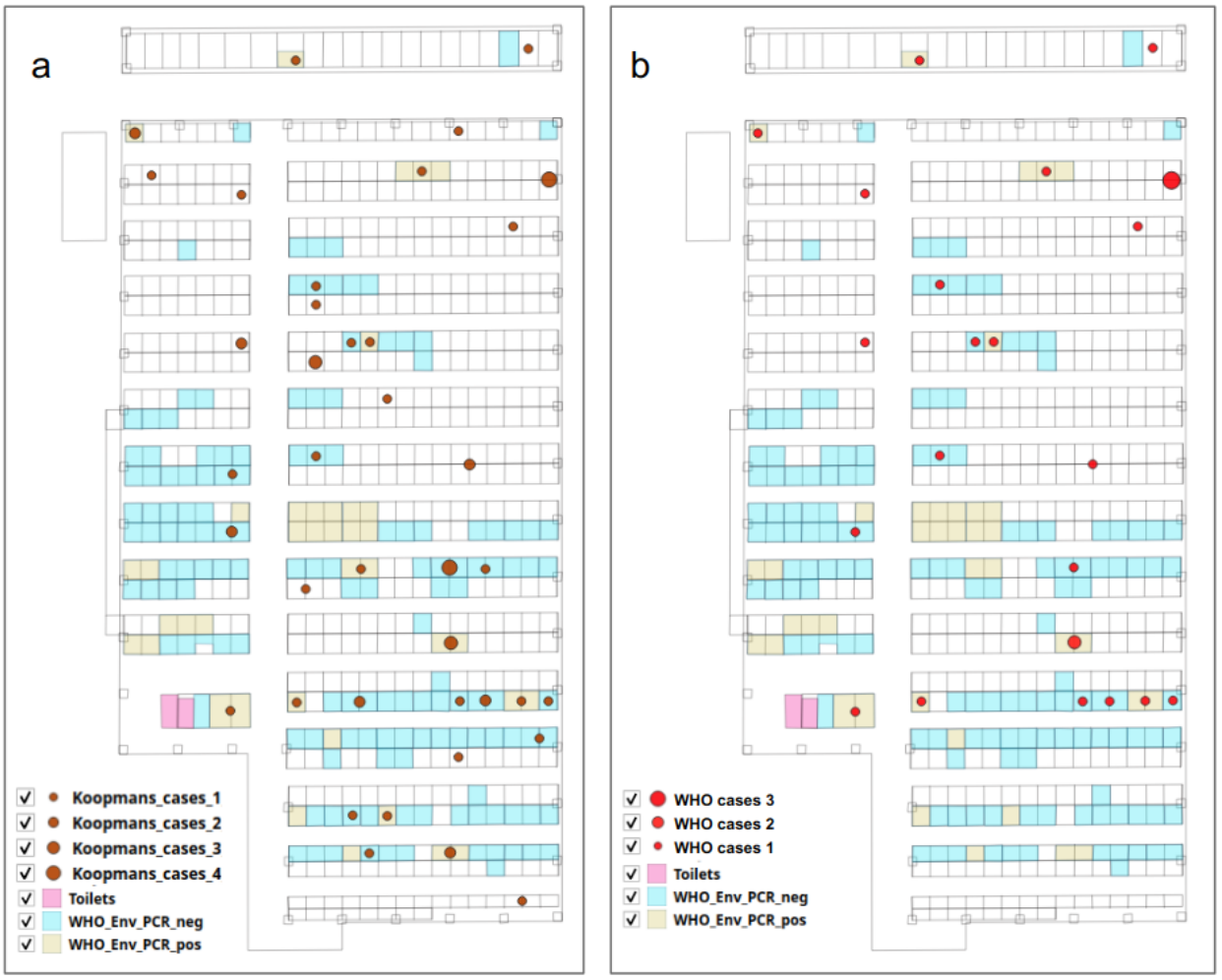

Supp. Fig. 9. COVID-19 cases with fixed stalls in the Western section of the market (Koopmans, 2021) and COVID-19 cases in the Western section of the market after Joint WHO-China Study (2021a,b).

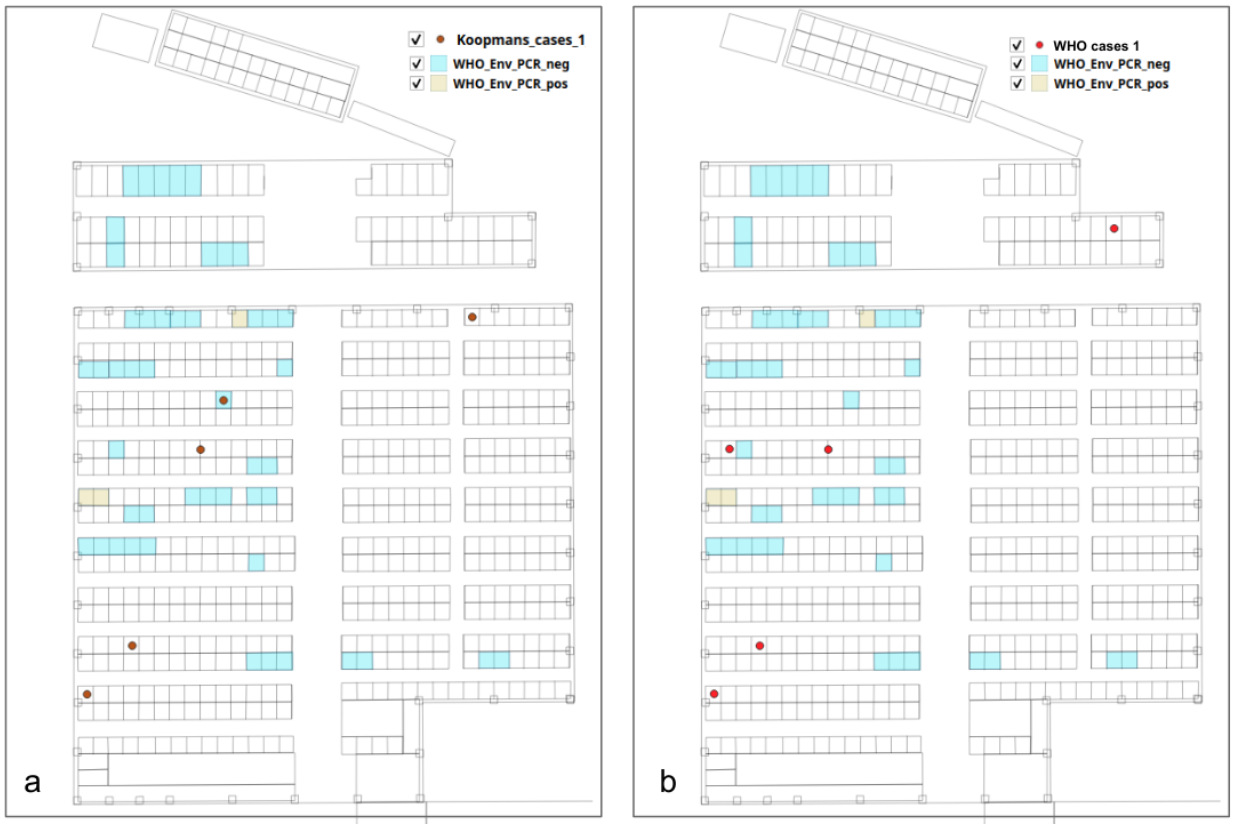

Supp. Fig. 10. COVID-19 cases in the Eastern section of the HSM. a) COVID-19 cases with fixed stalls in the Eastern section of the market after Koopmans (2021) and b) COVID-19 cases in the Eastern section of the market after Joint WHO-China Study (2021a,b).

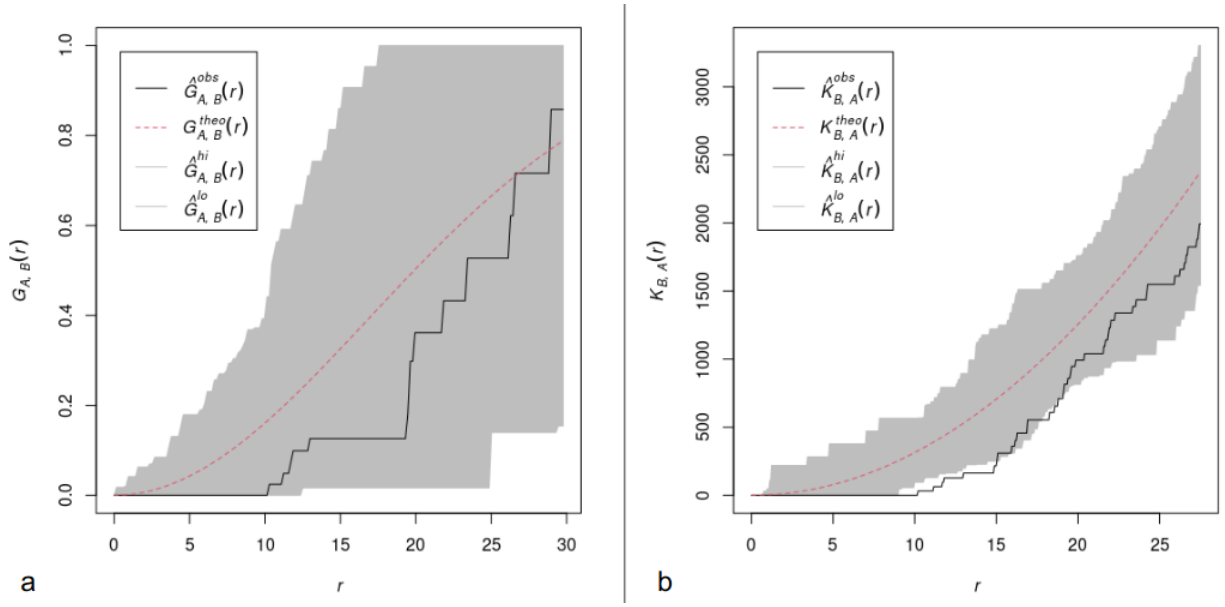

Supp. Fig. 11. Analysis of cases and wildlife stall locations in the Western section of market only using Ripley's cross functions in spatstats (Baddeley and Turner 2005). COVID-19 cases as per Koopmans (2021). a) Simulation (39 runs) of $G_{cross}(A,B)$ function representing the distribution of the distance from case location (A) to the nearest wildlife stall (B); b) Simulation (39 runs) of $K_{cross}(B,A)$ function representing $1/\lambda_A$ times the expected number of cases (A) within a distance r of a typical wildlife stall point (B), where λ_A is the density (intensity) of COVID-19 cases.

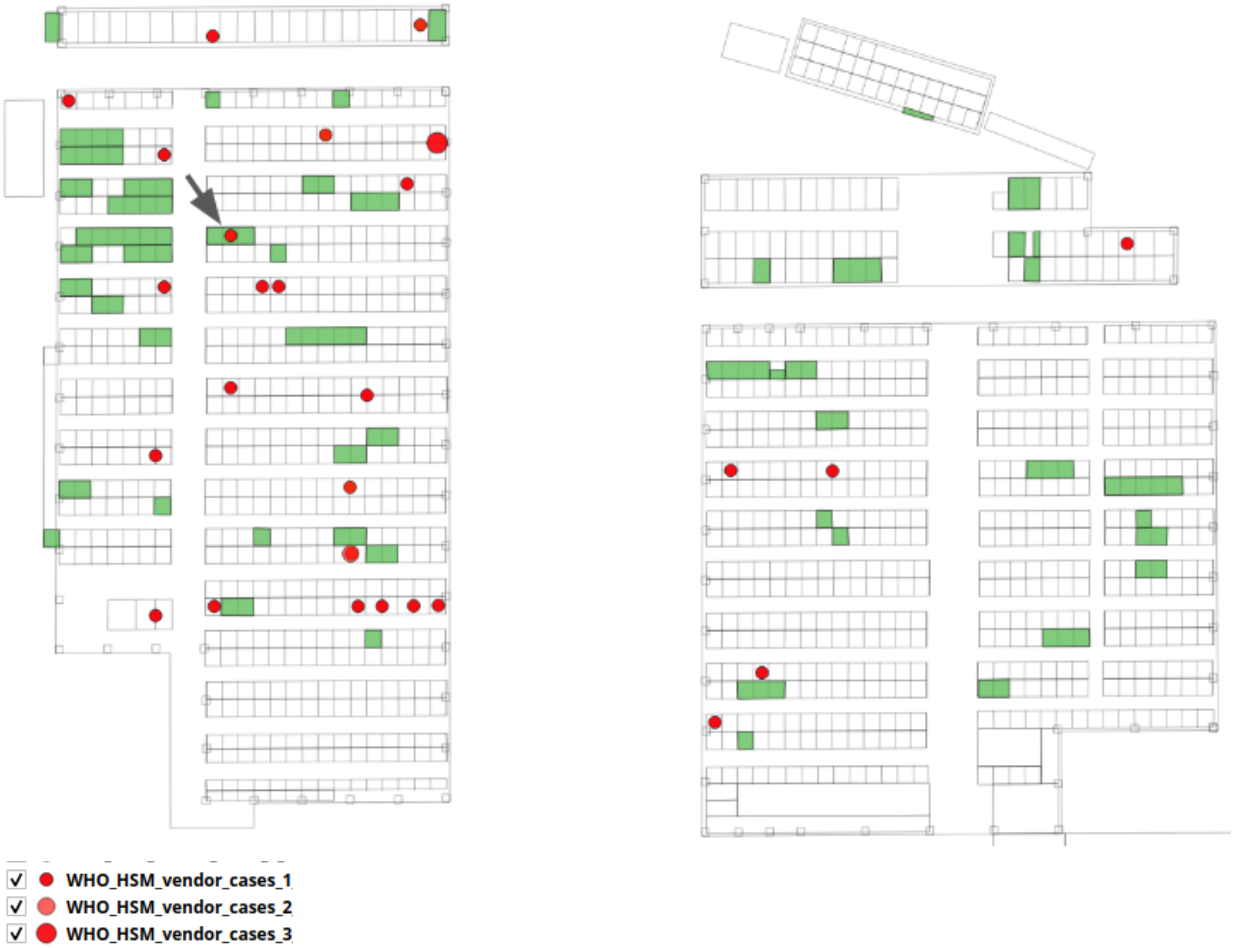

Supp. Fig. 12. Location of vegetable stalls and COVID-19 case locations from week ending 31 December 2019. First case location (black arrow), was located at a stall classified as a vegetable stall in the Western area of the market by the Joint WHO-China Study (2021a,b).

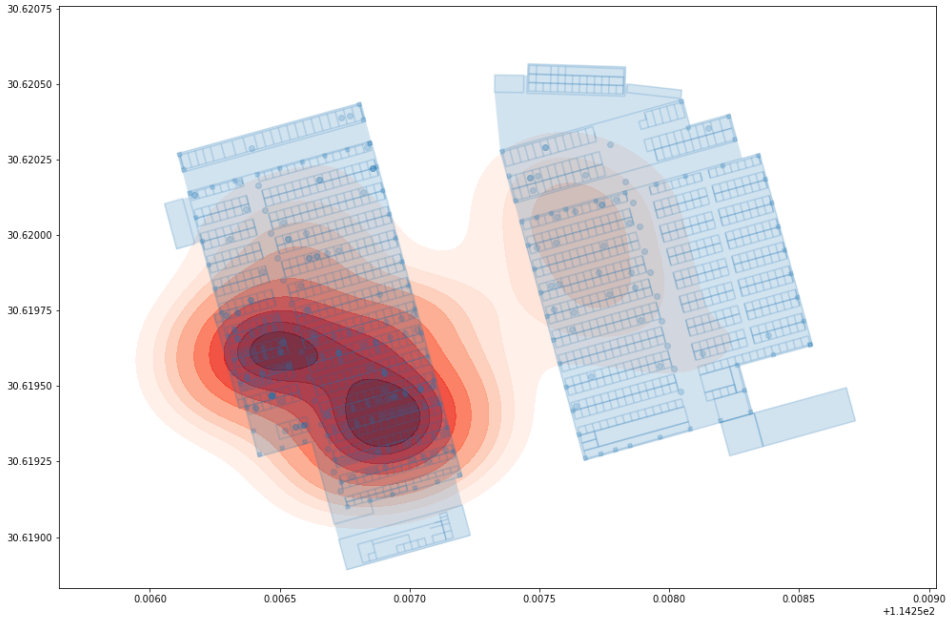

Supp. Fig. 13. KDE plot of Location of PCR negative environmental samples taken at the HSM. Data sourced from Worobey et al. (2022b).

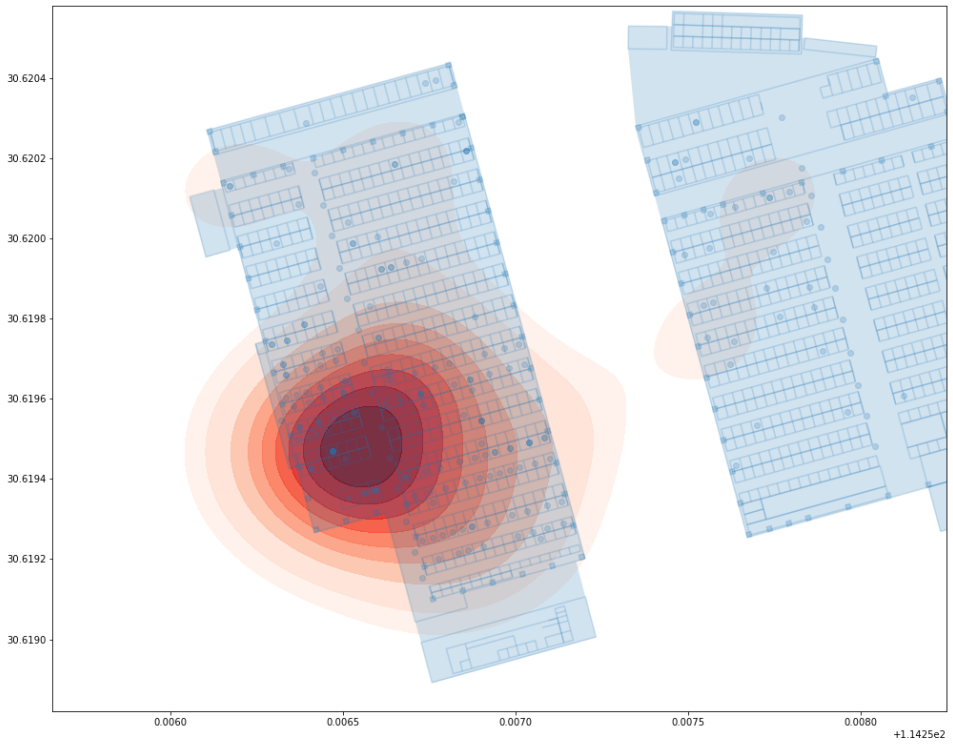

Supp. Fig. 14. KDE plot of Location of PCR positive environmental samples taken at the HSM. Data sourced from Worobey et al. (2022b).

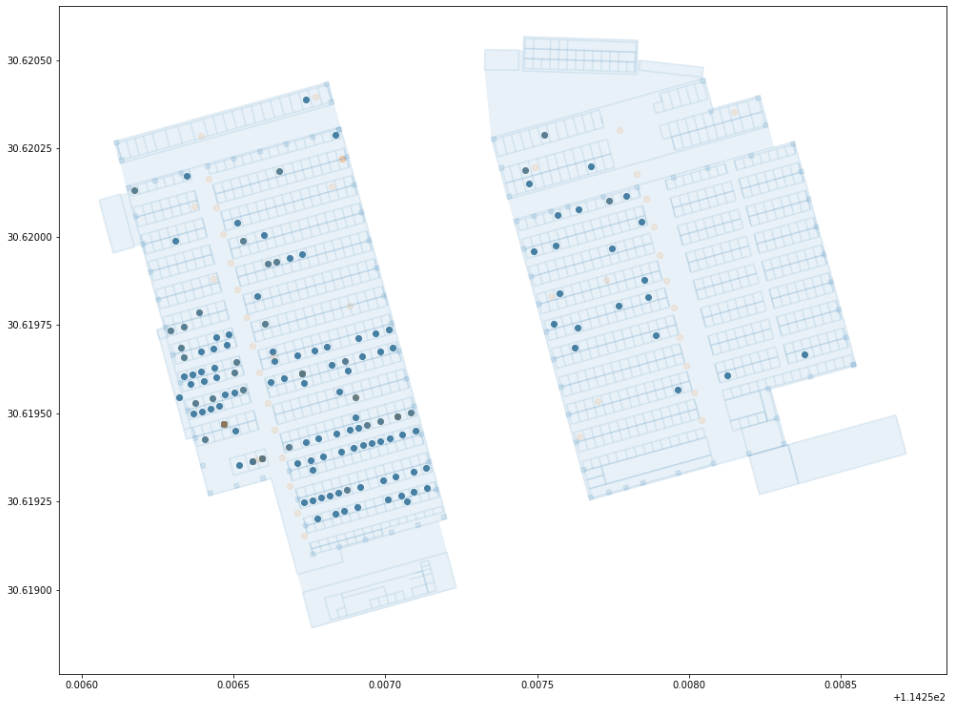

Supp. Fig. 15. Location of environmental samples taken at the HSM. Data sourced from Worobey et al. (2022).

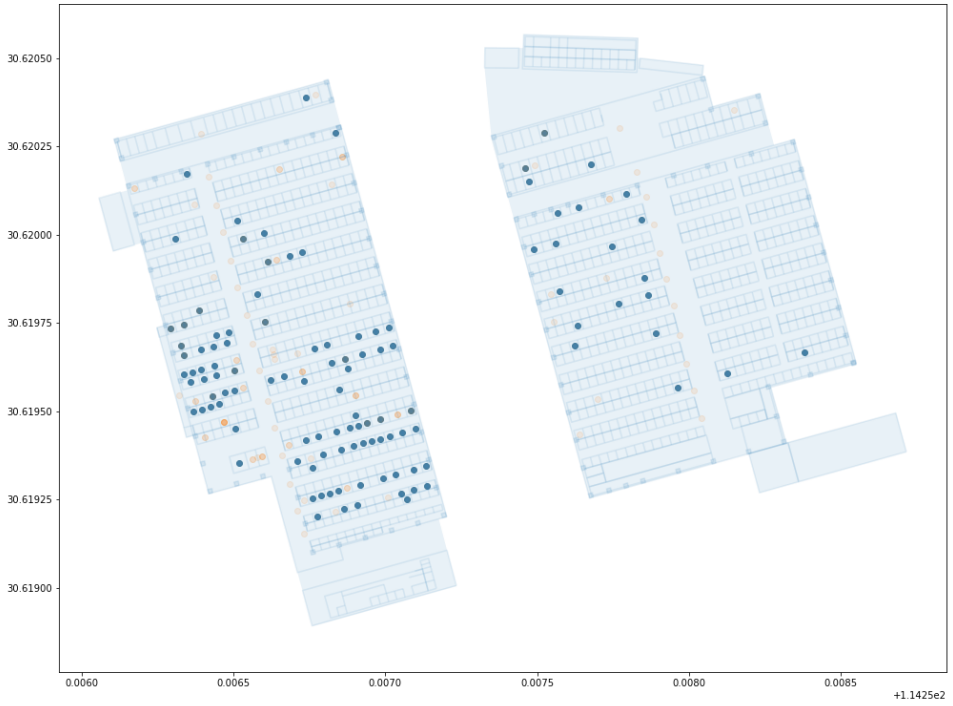

Supp. Fig. 16. Location of PCR negative environmental samples taken at the HSM. Data sourced from Worobey et al. (2022b).

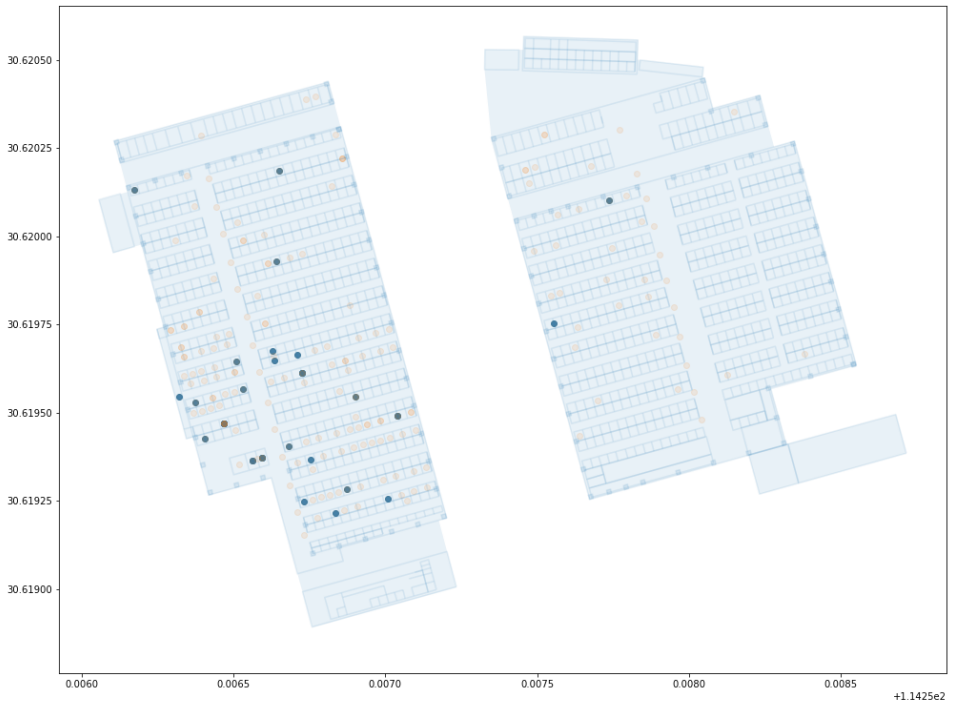

Supp. Fig. 17. Location of PCR positive environmental samples taken at the HSM. Data sourced from Worobey et al. (2022b).

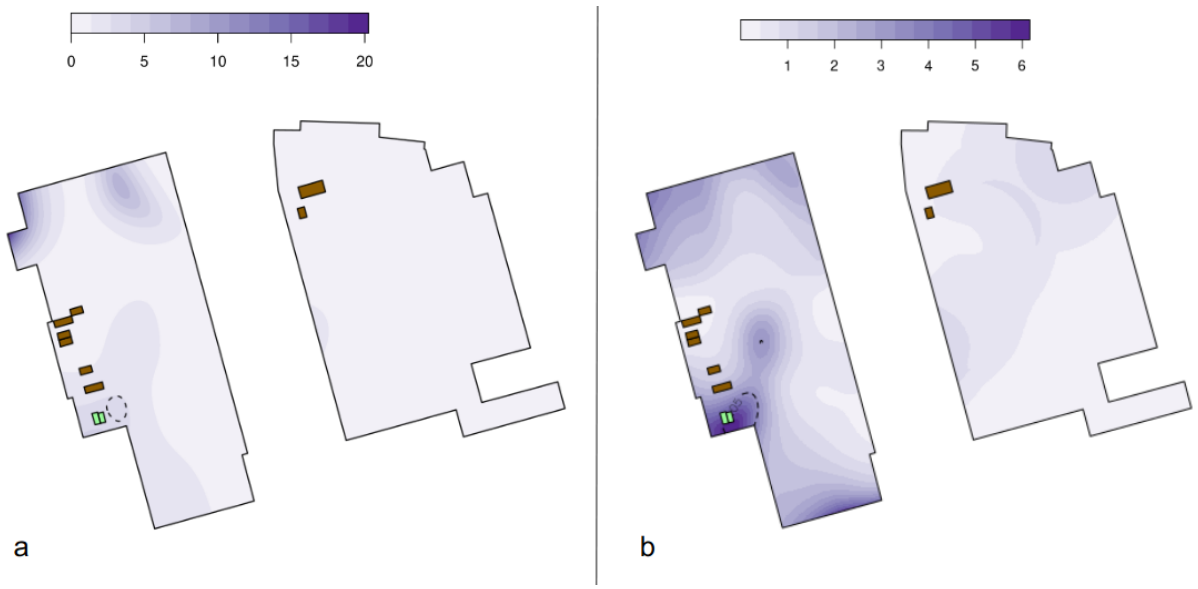

Supp. Fig. 18. Relative risk analysis of environmental positive samples using sparr (Davies et al. 2018). a) Ratio of the environmental positive density to control density (environmental negative) using deduplicated samples and default adaptive smoothing=False; b) Ratio of the environmental positive density to control density (environmental negative) using deduplicated samples and adaptive smoothing. Statistically significant elevated risk regions indicated by dashed contours.

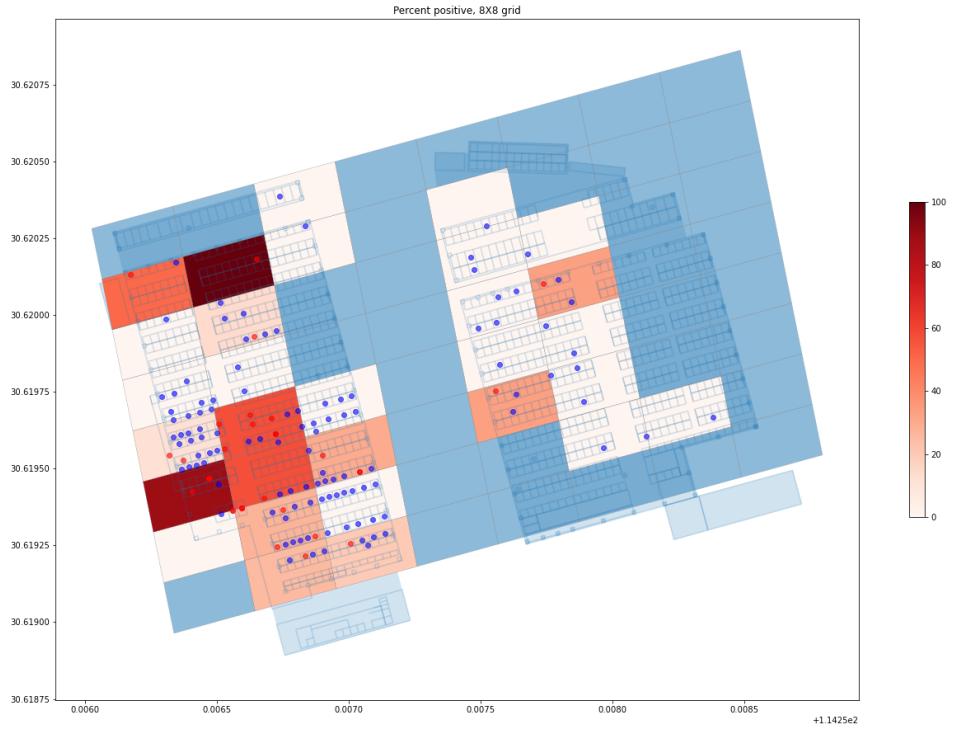

Supp. Fig. 19. Positive environmental samples as a percentage of total environmental samples per grid cell for a 8X8 cell grid over the HSM.

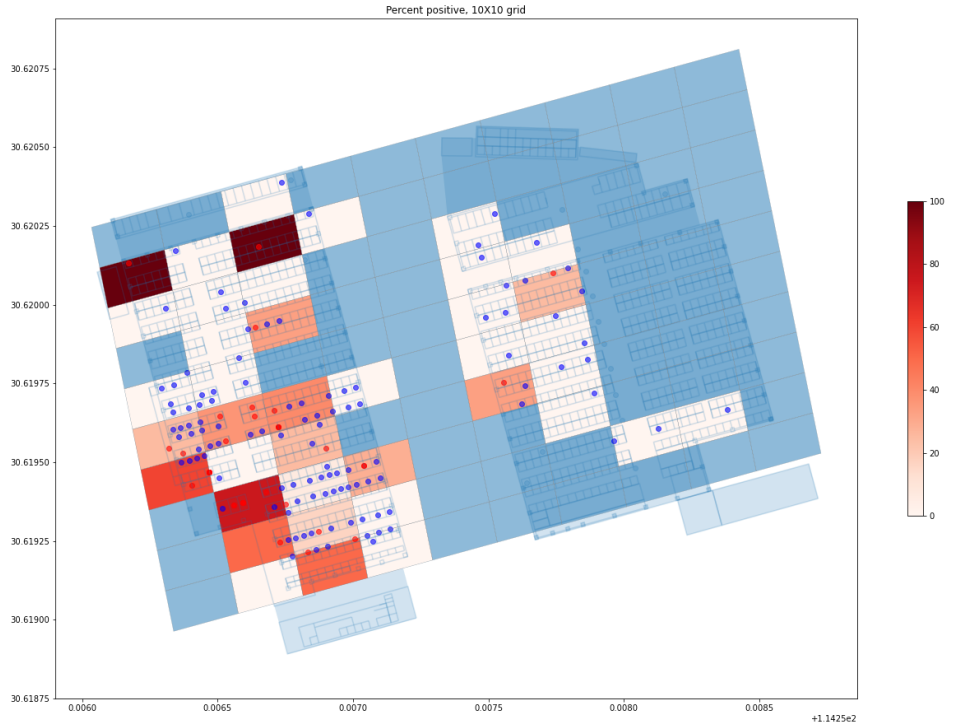

Supp. Fig. 20. Positive environmental samples as a percentage of total environmental samples per grid cell for a 10X10 cell grid over the HSM.

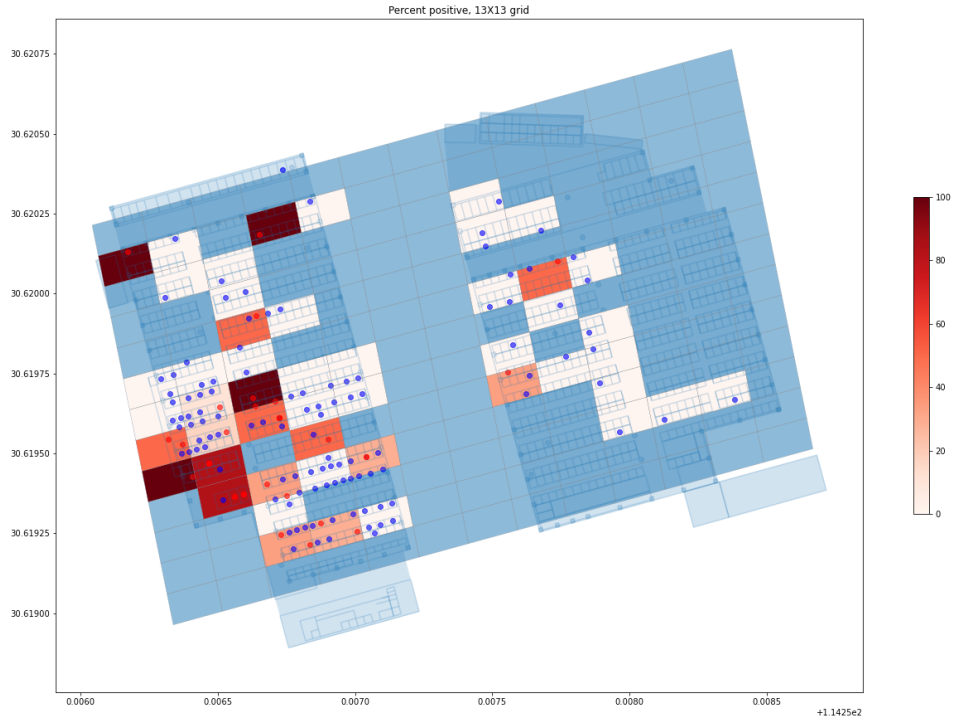

Supp. Fig. 21. Positive environmental samples as a percentage of total environmental samples per grid cell for a 13X13 cell grid over the HSM.

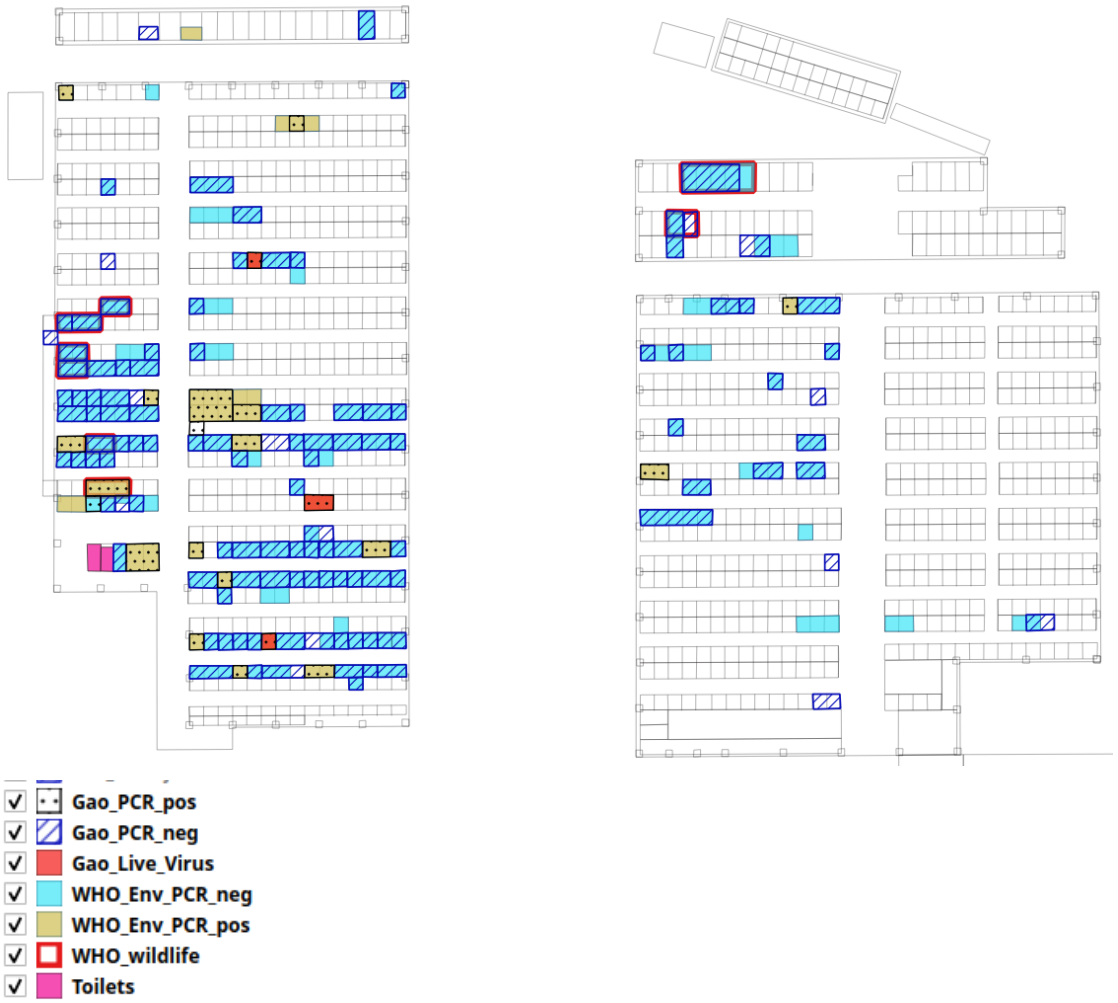

Supp. Fig. 22. Multiple differences are noted between environmental sampling published by Joint WHO-China Study (2021a,b) and Gao et al. (2022).

Stall Figures

Supp. Fig. 23. Stall West 8/25 (on right) as filmed in July 2019. After Babarleelehant (2021). See Fig. 11 for location.

Supp. Fig. 24. Stall West 8/25 (on left) as filmed in 2018 . After Babarleelehant (2021). See Fig. 11 for location.

Supp. Fig. 25 a,b. Stall West 8/25 as filmed on 31 December 2019 (closed door in the middle). After Babarleelehant (2021). See Fig. 11 for location.

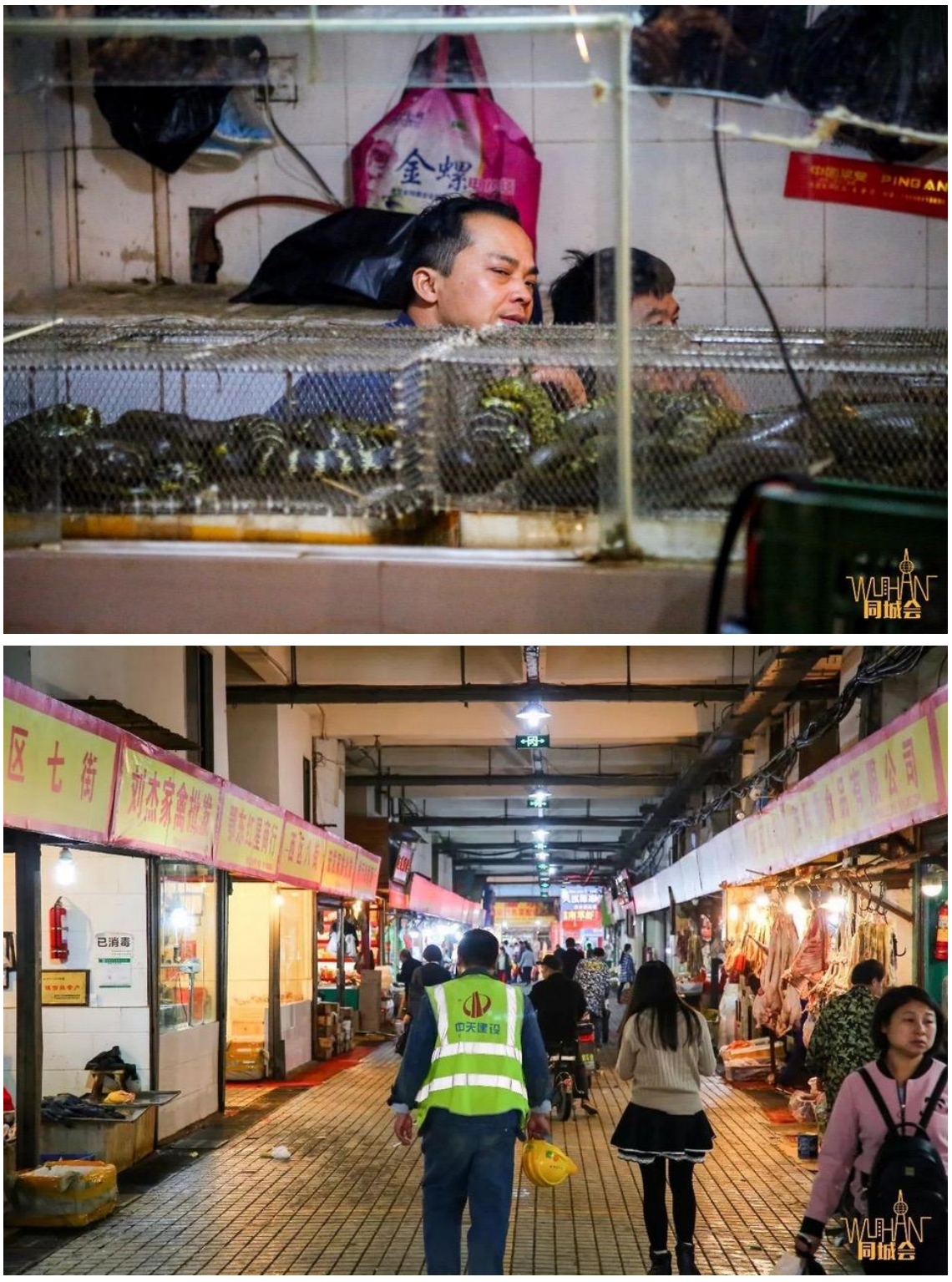

Supp. Fig. 26 a,b. Stall West 8/25 as photographed in 2017. (for b) location is on left). Only snakes were found in this stall from available photo and video evidence. After Babarleelehant (2021). See Fig. 11 for location.

Supp. Fig. 27. Stall West 8/19-23 West 7/20-24 “腊味香食品有限公司”, a seller of preserved and fresh livestock meat or “腊肉”with pig carcasses hanging at corner. After Babarleelehant (2021). See Fig. 11 for location.

Supp. Fig. 28. Stall West 8/19-23 West 7/20-24 captured on video in July 2019. Large freezers can be seen inside the stall. After Babarleelehant (2021). See Fig. 11 for location.

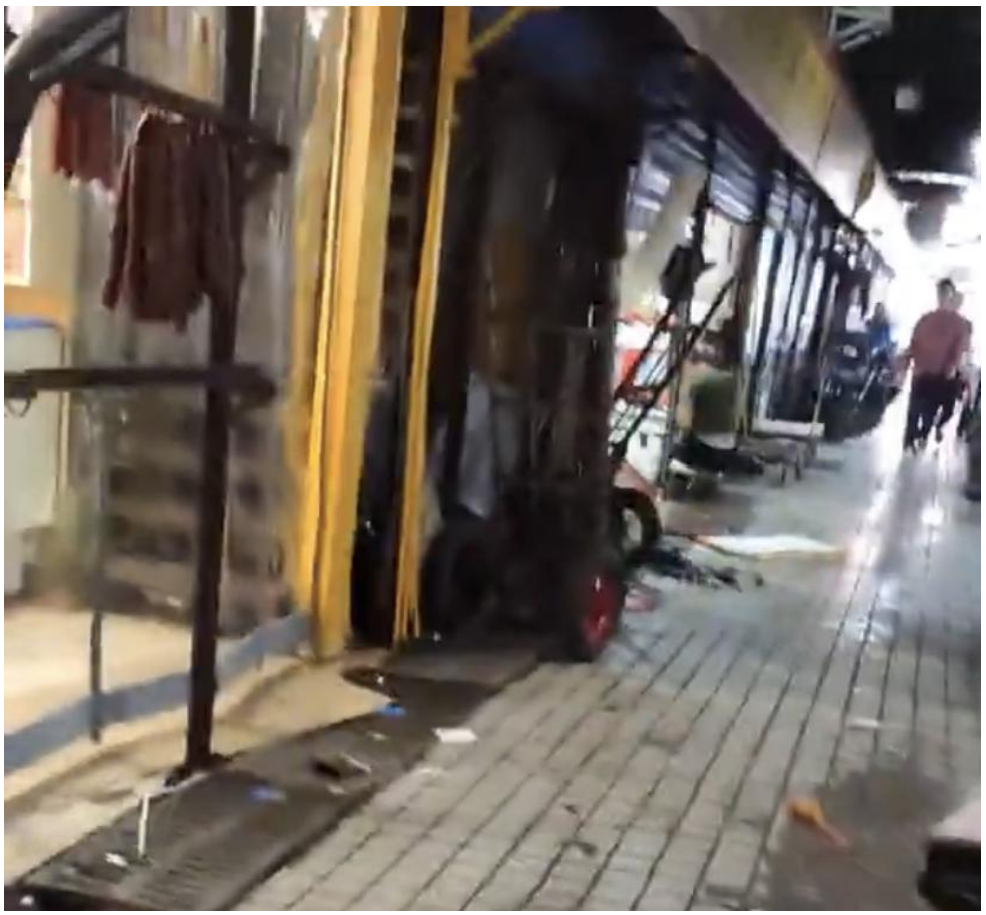

Supp. Fig. 29. A possible staircase leading upstairs can be seen inside stall West 7/20-24 West 8/19-23. After Babarleelehant (2021). See Fig. 11 for location.

Supp. Fig. 30. Stall West 7/25 “荣昌冻品” on right of image (with green freezer in front). The stall is a frozen food stall, no evidence of wild animals is evident. After Babarleelehant (2021). See Fig. 11 for location.

Supp. Fig. 31. Stall West 7/25 “荣昌冻品” on left of image (green freezer in front). On right hand side is a view to the West down 7th street. West 7/31-33 is the third and fourth stall opening when counting from West 7/25 along 7th street. West 7/35-37 is the fifth and sixth stall opening. Note, Fig. 3 B in Worobey et al. (2022a) was likely taken between West 7/29 and West 7/31, looking towards West 7/31. Here in December 2019, no animal cages (which are routinely placed by vendors outside stalls) can be seen outside West 7/31-33 or West 7/35-37. After Babarleelehant (2021). See Fig. 11 for location.

Supp. Fig. 32. View to the West down 7th street. Stall West 7/25 "荣昌冻品" at front left of image. West 7/26-28 can be seen on the right. After Babarleelehant (2021). See Fig. 11 for location.

Supp. Fig. 33 a,b. Stall West 6/29-33 as filmed from the perspective of the store room at the western end of street 6 (Western section of HSM), looking East, on 31 December 2019. See closed doors, third from left of open stall. Although clearly closed, no cages are evident. After Babarleelehant (2021). See Fig. 11 for location.

Supp. Fig. 34. Looking West along 5th street. Stalls West 5/32 and West 5/34 are located behind the environmental worker. Stalls West 5/36 and West 5/38 do not have a sign and it is unclear if these stalls were occupied in December 2019. West 5/26-34 is named "志翔冻品商行" (Zhixiang Frozen Products) and sold frozen meat. After Babarleelehant (2021). See Fig. 11 for location.

Supp. Fig. 35 a-d. Stall West 7/15-17 as filmed in July 2019 (after Babarleelehant, 2021). No cages containing live mammals are evident. After Babarleelehant (2021). See Fig. 11 for location.

Sample A20

The Ct value of real time PCR (quantitative PCR or qPCR) represents the number of PCR cycles at which the reaction curve intersects a threshold value. A higher Ct value indicates that less nucleic acid was present in the sample (Supp. Fig. 36). From HSM environmental sampling, SARS-CoV-2 was only able to be isolated from the three samples with a Ct value <30 (Supp. Fig. 37). Notably, of these, the two samples with lowest Ct values were sampled from stalls with confirmed COVID-19 patients (Gao et al., 2022). Since the Ct value is highly correlated with nucleic acid abundance, an expected read depth at positions 8782 and 28144 (Gao et al. 2022) can be calculated based on sample titer genome copies. As shown in Supp. Table 1, we would have expected sample A20 with a Ct value of 32.48 to have read depth between that for sample F46 (Ct value of 31.8) and F98 (Ct value of 35). However this is not the case.

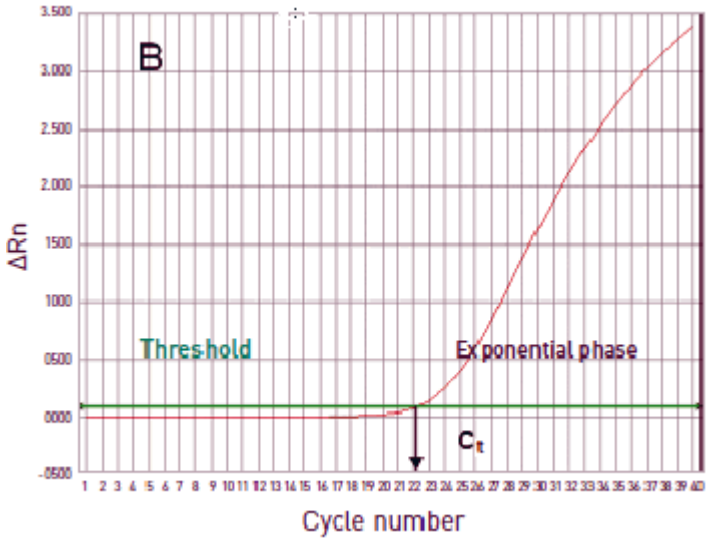

Supp. Fig. 36. Fluorescence above baseline (ΔRn) plotted against PCR cycle number. Ct is the cycle value where the PCR curve crosses a threshold value. After ThermoFisher Scientific https://www.thermofisher.com/au/en/home/life-science/pcr/real-time-pcr/real-time-pcr-learning-center/real-time-pcr-basics/real-time-pcr-understanding-ct.html

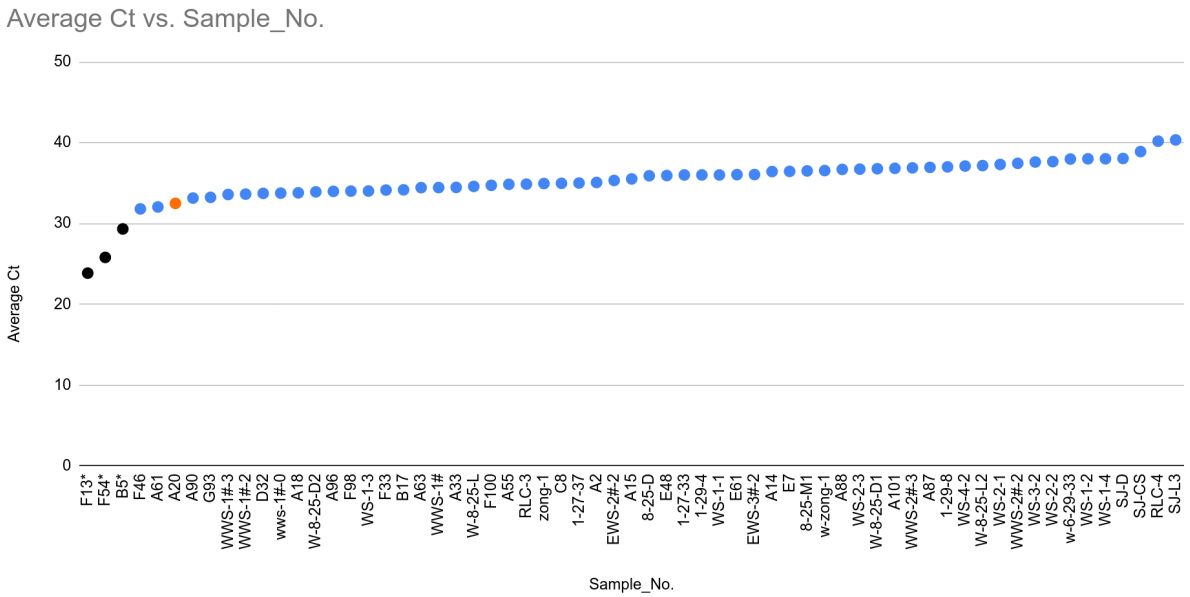

Supp. Fig. 37. Ct value (averaged for samples C8,SJ-D,SJ-CS,SJ-L3,RLC-4,RLC-3) per sample. SARS-CoV-2 was isolated from samples F13, F54, and B5 which all had a Ct value <30 (black). Sample A20 is shown in orange. Based on data in Gao et al. (2022).

Position	8782				28144				PCR
	A	T	C	G	A	T	C	G	Ct
F13*	5	10	1874	3	0	1669	0	0	23.85
F54*	1	1	106	0	1	39	0	0	25.8
B5*	0	0	86	0	0	85	0	0	29.32
F46	0	0	1	0	0	0	0	0	31.8
A61	0	0	2	0	0	0	1	0	32.04
A20	7	359	1	0	1	5	1596	5	32.48
F98	0	0	20	0	0	3	0	0	34
A33	0	0	2	0	0	0	1	0	34.46
A88	0	0	0	0	0	2	0	0	36.69
A87	0	0	0	0	0	1	0	0	36.94

Supp. Table 1. Summary of number of reads mapped to positions 8782 and 28144 in different samples and their PCT Ct values after Gao et al. (2022) Extended Data Table 2 and Table 1. * samples where SARS-CoV-2 was isolated.

We see an inverse correlation between read depth and Ct for the three samples where viral isolation was successful, samples F13, F54 and B5 (Supp. Table 1). For the samples where viral isolation failed, other than sample A20, F98 exhibited the highest coverage at positions 8782 and 28144 with no other samples (other than A20) having significant coverage on 8782 and 28144.

Sample A20 is clearly anomalous in that it has a moderate Ct value, yet has the second highest coverage at positions 8782 and 28144 of all samples (Supp. Table 1).

We can extrapolate from sample F98 an upper bound of 20*(2^(34-32.48))=58 reads at position 8782 for samples where viral isolation failed. Extrapolating from sample B5 gives an upper bound of 86*(2^(29.32-32.48))=10 reads on 8782 for samples where viral isolation succeeded. We can thus approximately define a range for which the number of reads covering position 8782 may be expected for a sample with qRT-PCR Ct of 32.48 using the particular sequencing protocol for this particular batch of samples (DNBSEQ-T7). We note however, the A20 genome has a read depth of 359 at 8782 which is 6.18 times higher than the estimated upper bound to read coverage for a sample with a qRT-PCR Ct value of 32.48 calculated above (i.e. 58 reads).

Similarly, for position 28144, extrapolating from sample F98 gives an approximate upper bound of 3*(2^(34-32.48))=9 reads at position 28144 for samples with a qRT-PCR Ct value of 32.48 and where viral isolation failed. Extrapolating from sample B5, we can estimate an approximate upper bound of 85*(2^(29.32-32.48))=10 reads at position 28144 for samples where viral isolation succeeded, can can estimate an approximate range for expected read depth at position 28144 for a sample with qRT-PCR Ct number of 32.48 (using DNBSEQ-T7 and the specific sequencing protocol for this batch of samples). However, A20 has a coverage of 1596 at 28144 which is 159.6 times higher than expected.

Curiously, for all the samples that have significant read coverage depths at positions 8782 and 28144, the number of reads covering 8782 is greater than the number of reads covering 28144, whereas in sample A20, the number of reads covering 28144 is greater than the number of reads covering 8782.

Additionally, sample A20 is the only sample where a complete viral genome was obtained yet no live virus was isolated. Using a correlation analysis, Quay (2022) concluded that the lineage A/S reads in A20 was a statistical outlier (Supp. Fig. 38), with a potential source of the anomaly being post-sampling contamination. However the lineage B/L fraction in sample A20 was consistent with that expected from the qRT-PCR Ct value (Quay 2022).

Given these anomalies we cannot exclude the possibility that the lineage A SARS-CoV-2 genomes within sample A20 may have been introduced to the high-throughput sequencing library before genome sequencing took place but after the qRT-PCR reaction and the virus isolation attempt took place.

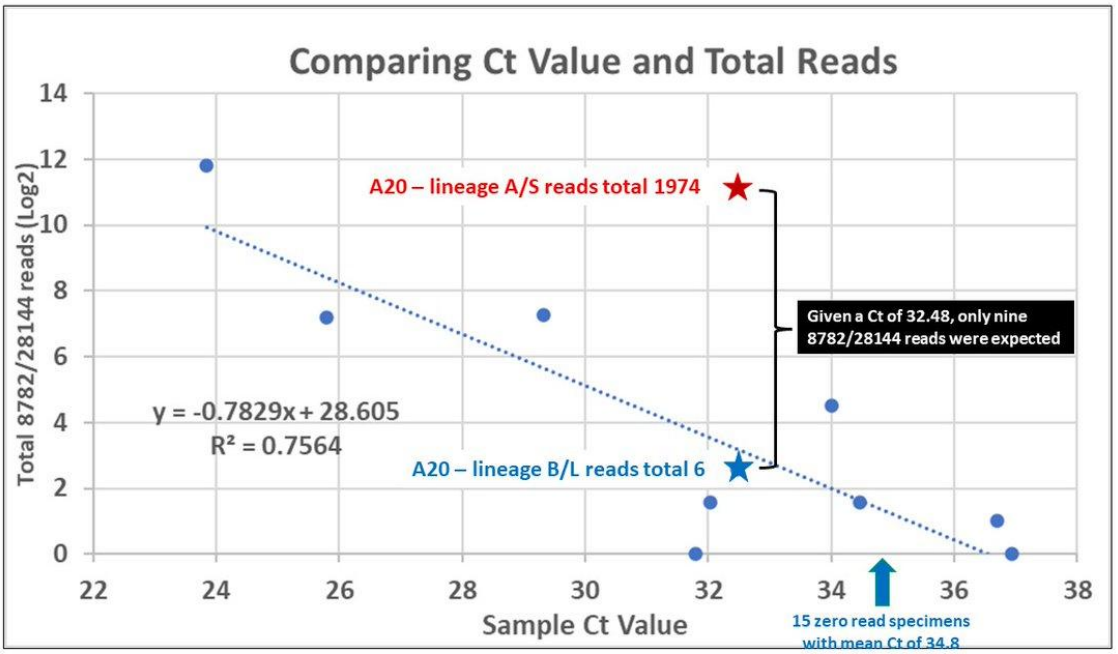

Supp. Fig. 38. Log_2 of the total sequencing depth at 8782/28144 in all sequenced Huanan market environmental samples plotted against the qRT-PCR Ct value of each sample. After Quay (2022).

As the qRT-PCR process is an exponential amplification process, the Ct value denotes the number of cycles it takes to exponentially amplify the RNA target in the sample to a set concentration that is then detected by the PCR machine, it is expected that the Ct value of a sample to be linearly and inversely correlated to the original concentration of the RNA template within the sample, which is directly correlated to the sequencing depth of the sample, with each multiplication in the concentration of the original RNA sample by the single cycle amplification efficiently (which is close to 2, the ideal condition) of the qRT-PCR setup being expected to reduce the qRT-PCR Ct value by roughly 1.

Plotting the log_2 of the sequencing depth at 8782 and 28144 of each environmental sample against their Ct values reveals that for all samples, including the lineage B fraction in sample A20 (the alignment depth with C8782 and T28144) show an inverse linear correlation as expected, with a correlation factor being close to -1 as expected from the exponential amplification process of qRT-PCR.

The lineage A alignment within sample A20 however is found to be a statistical outlier with an absolute standard residual of 3.4 when this correlation is considered, compared to the maximal standard residual level of 1.3 for other points on the graph, including the number of lineage B alignments at 8782 and 28144 within sample A20.

Mutations

Sample A20 carried 2 additional mutations: C6145T and G26262T (Supp. Fig. 39). Both mutations have been found in isolates of SARS-CoV-2 in humans, whereas while C6145T is of uncertain ancestry due to it being a hypervariable site in Sarbecovirses (both C and T

have been found in closely related genomes of the same clade, such as BANAL-52, BANAL-103, BANAL-116, BANAL-236 and BANAL-247, RaTG13, RacCS203 and RpYN06, making it difficult to say for certain whether C6145 or T6145 was present in the immediate ancestor of SARS-CoV-2). G26262T is not found in any other Sarbecoviruses, which makes it a novel site and clearly non-ancestral (Supp. Figs 40-41).

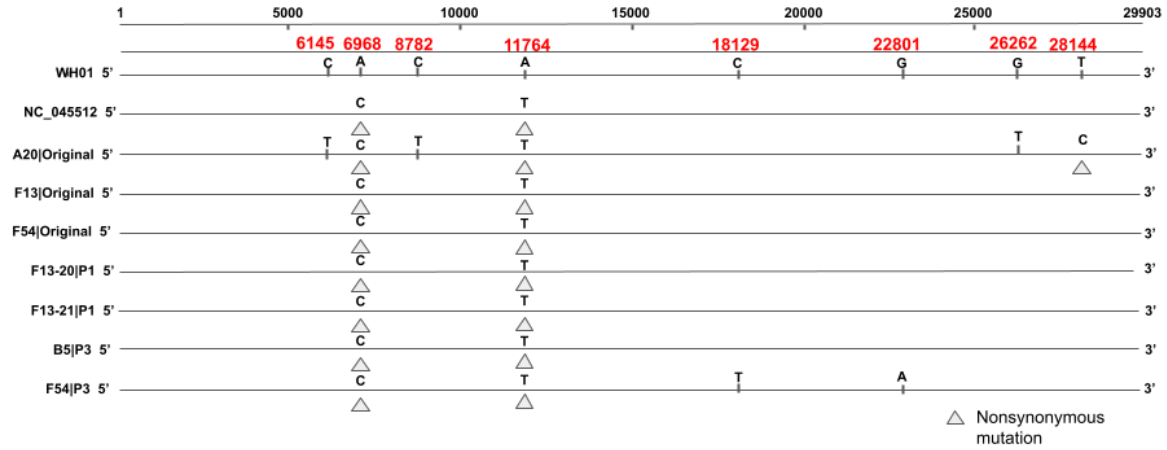

Supp. Fig. 39. Alignment of complete SARS-CoV-2 genomes assembled from HSM environmental samples, after (Gao et al. 2022).

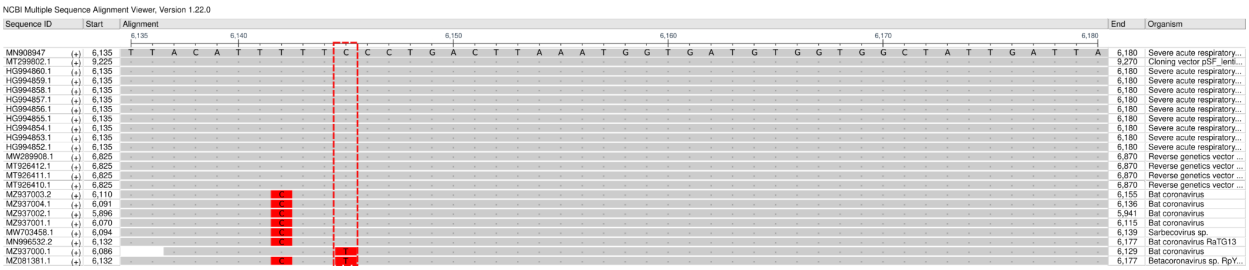

Supp. Fig. 40. Closest SARSr-CoVs to SARS-CoV-2 Wuhan-Hu-1 (MN908947) in 6135-6180 region using blastnt excluding SARS-CoV-2 and synthetic constructs. Position 6145 is highlighted in red box and is a variable site in sarbecoviruses.

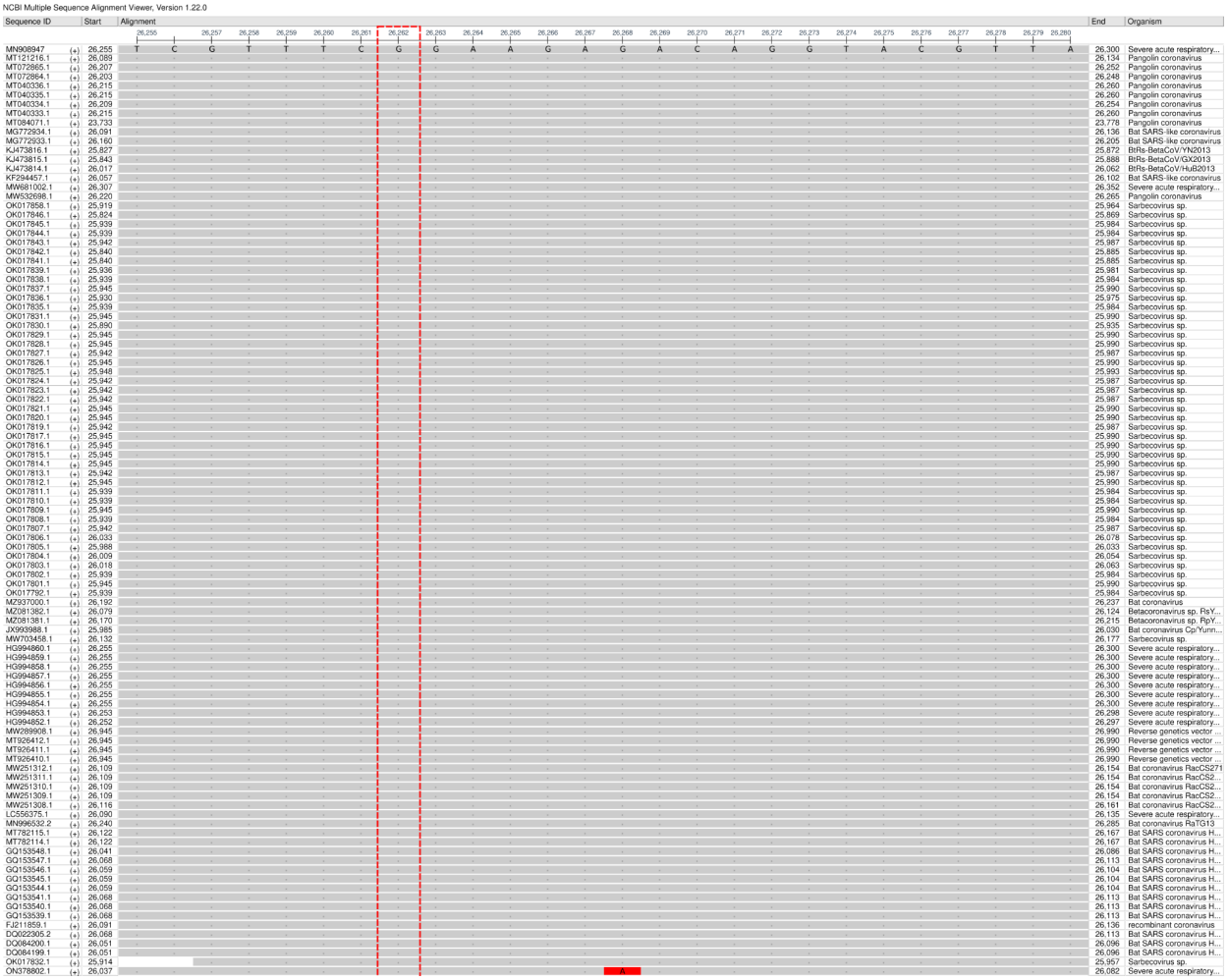

Supp. Fig. 41. 100 closest SARSr-CoVs to SARS-CoV-2 Wuhan-Hu-1 (MN908947) in 26255-26300 region using blastnt excluding SARS-CoV-2 and synthetic constructs. G26262 highlighted in red box is conserved across all searched sarbecoviruses.

While C->T transitions frequently happen in poorly sequenced genomes of SARS-CoV-2 due to the frequent deamination of cytosine both by RNA editing enzymes and by non-enzymatic processes during RNA degradation, G->T transversion happens mainly through oxidative stress in human airway cells and is considered to be a feature that is uniquely found for human isolates of SARS-CoV-2, requiring some level of passage in a human airway (Roy et al. 2020). 8-oxoguanine generated by reactive oxygen species has been shown to lead to G-T mutations (Ohno 2014). As we also observe two mutations C18129T and G22801A forming after three passages in VERO E6 cells of the isolated sample F54 compared to the original, it can not be ruled out that the mutations we see in A20 was the result of cell culture-associated mutations from a cell cultured isolate of lineage A SARS-CoV-2 of indeterminable (but likely type-strain) origin contaminating the library as it was being sequenced.

Read Depth

The environmental sample A20 deposited on GISAID by Gao et al. (2022) has 2 "N"s within 60nt of 28144 (Supp. Fig. 42), which is below the length of the average Illumina read which is typically 100 or 150nt. Gao et al. discuss that position 28144 has been sequenced to a coverage of 1596X. This indicates either a sudden increase in coverage with many reads ending between 28091 and 28144 or base calls at 28090 and 28091 containing similar amount of all four nucleotides at the location (as opposed to two or three which are assigned R,Y,W,S,M,K or B,D,H,V). This may be caused by amplicon contamination or cross-sample contamination by cell cultured strains of SARS-CoV-2. However, due to the unavailability of the raw data, it is impossible to deduce the exact scenario.

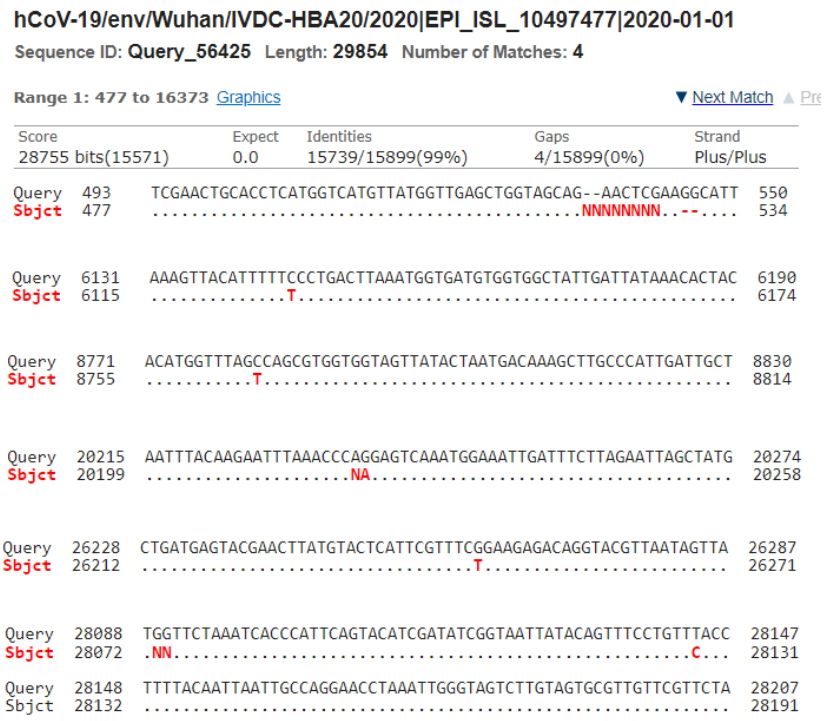

Supp. Fig. 42. Alignment of sample A20 (EPI_ISL_10497477) to SARS-CoV-2 (NC_045512.2).

It is worth mentioning that the sample F54 accumulated two mutations compared to the original at the third passage in VERO E6 cells. We cannot rule out the possibility, however unlikely, that contamination by cultured SARS-CoV-2 sequences within the same laboratory during the sequencing of sample A20 in 2021 could have led to the appearance of mutations C6145T and G26262T within the final assembled genome. Access to raw data is important to confirm all samples.

As discussed previously, we urge Gao et al. (2022) to review sample A20 in light of our findings to determine if our concerns are warranted. Making the raw NGS dataset available will allow validation of lineage A in the A20 environmental sample, rather than via potential cross-contamination from other sequencing runs.

PPE

The potential significance of PPE-related terms in regards to collection of samples A18-A20 is not discussed in Worobey et al. (2022b) and we expand on these terms. Samples A18 and A20 were taken from stall West 7/17,18 (Fig. 11), and with one other sample, A2, have two unique sample definitions in Chinese CDC report 2020 No. 53: "Shoe covers and soles" (鞋套鞋底) for A18 and "Gloves" for A20 (Epoch times, 2020). Although it is plausible that waterproof boots may have been left at stalls, we speculate that shoes are unlikely to have been left available for sampling, given the non-sanitary condition of the ground inside a wet market. In addition, as waterproof boots are already resistant toward sewage and offal penetration, wearing shoe covers over such boots would be redundant.

We note that there is no "cover" to a shoe and there is no "sole" to a shoe cover, whereas the sole means the bottom of a shoe and a shoe cover is a type of cover worn over the shoes typically by disinfection workers and epidemic control staff as a part of their personal protective equipment (PPE). For sample A18 "Shoe covers and soles" to count as one sample, implies the shoe cover was on the shoe at the time of sampling (Fig. 47), it is thus unclear if an investigators' own PPE or if a vendors shoe was sampled.

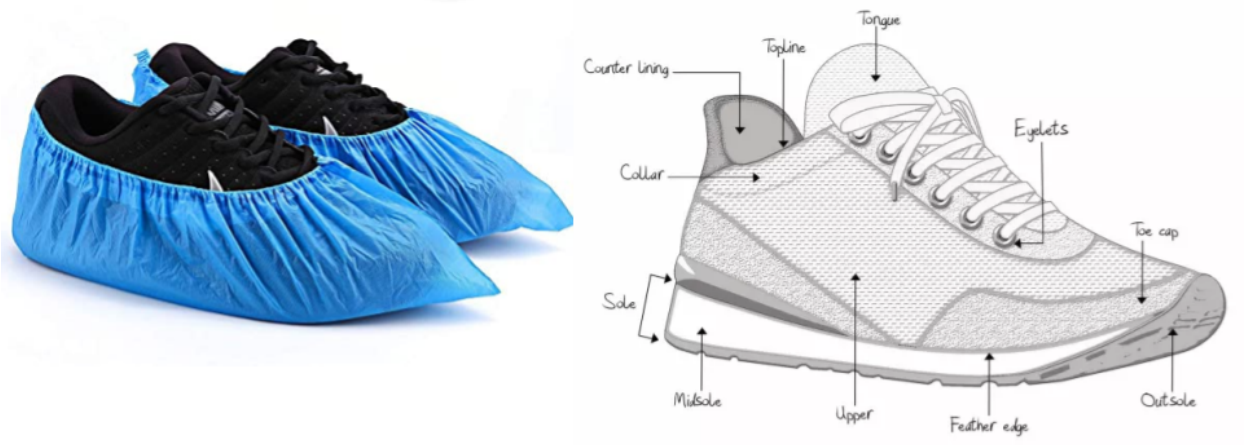

Supp. Fig 43. A Shoe cover and names for different parts of a shoe.

As gloves are also part of the investigators' own PPE, it is unknown if sample A20 similarly referred to a sample taken from the PPE of an investigator, potentially at the end of a sampling collection round.

We notice that the sampling of gloves (glove prints, glove tips) appears to be a standard method of environmental microbial monitoring (Boom 2020; Technical Safety Services, 2022). We also note that specialized "boot cover swab kits" (or "shoe cover swab kits") were sold for the specific purpose of pathogen sampling and testing by certain suppliers (Romer labs, 2022).

The significance, if samples A18 and A20 were sampled from disinfection/environmental samplers shoe covers and or gloves respectively, is that the SARS-CoV-2 RNA could have come from anywhere in the market.

Animal Testing and Susceptibility

Common name	Species	HSM animals tested	Experimental IP/Entry/Binding Energy	Live infection/transmission	Found in wild	In silico risk	Summary
Hog badger	Arctonyx albogularis	(Badger) 6	IP (S1/RBD): Trace (Zhao et al. 2020); Pseudotyped entry: Low/Medium (Zhao et al. 2020)		No		Unlikely
Asian badger	Meles leucurus				No	1 very low (Mellivora capensis) (Karlssonlab 2022/Damas et al. 2020)	Unlikely
Pallas squirrel	Callosciurus erythraeus				No		Unknown
Amur Hedgehog	Erinaceus amurensis	16	(european hedgehog) Binding Energy: Nil (Wu et al. 2020)		No	Very low (Erinaceus europaeus) (Karlssonlab 2022/Damas et al. 2020); Unlikely to bind: Luan et al., 2020; Liu et al., 2020; Lam et al., 2020; Wu et al., 2020	Unlikely
Malayan procupine	Hystrix brachyura				No	2 low (Hystrix cristata) (Karlssonlab 2022/Damas et al. 2020)	Unlikely
Chinese hare	Lepus sinensis	52	(rabbit) IP (S1/RBD): Strong (Zhao et al. 2020); Pseudotyped entry: Medium/High (Zhao et al. 2020); Medium (Mykytyn et al. 2021); Binding Energy: (rabbit) High (Huang et al. 2020); High (Wu et al. 2020)	(rabbit) Yes (Mykytyn et al. 2021); (rabbit) Transmission: unable to support sustained intraspecies transmission (Mykytyn et al. 2021)	No	3 medium (Lepus timidus) (Karlssonlab 2022/Damas et al. 2020)	Possible
Marmot	Marmota himalayana				No	3 medium (Karlssonlab 2022/Damas et al. 2020); unlikeley Liu et al., 2020	Unknown

Chinese muntjac	Muntiacus reevesi	6		(Odocoileus virginianus (from Capreolinae, a different Subfamily)) (Cool et al. 2021)	No (nor C. elapus; Dama dama) (Moreira-Soto et al. 2022); No (Muntiacus reevesi; Dama dama; Cervus elaphus) Holding et al. (2022); only found in White tailed deer and Mule deer in North America (https://www.woah.org/app/uploads/2022/06/sars-cov-2-situation-report-13.pdf). Note the different C-terminus for US continental Odocoileus ACE2 relative to other Cervids (Cool et al. 2021) (https://www.ncbi.nlm.nih.gov/nucleotide/XM_020913306.1?report=genbank&log$=nucltop&blast_rank=1&RID=D60DWJT2016)	1 very low (Karlssonlab 2022/Damas et al. 2020)	Unlikely
Siberian Weasel	Mustela sibirica	1	(ferret) Binding Energy: High (Huang et al. 2020)	(ferret) upper respiratory tract only (Shi et al. 2020)	No	1 very low (Mustela erminea) (Karlssonlab 2022/Damas et al. 2020)	Possible
Coypu	Myocastor coypus				No	1 very low (Karlssonlab 2022/Damas et al. 2020)	Unknown
Mink	Neovison vison				Yes (Europe and Americas only, not Asia (https://www.woah.org/app/uploads/2022/06/sars-cov-2-situation-report-13.pdf))	1 very low (Karlssonlab 2022/Damas et al. 2020); Likely: Lam et al. 2020	Possible
Raccoon dog	Nyctereutes procyonoides		IP (S1/RBD): Trace (Zhao et al. 2020); Pseudotyped entry: Medium (Zhao et al. 2020); Binding Energy: Medium (as per Dog, lower than Cat (Wu et al. 2020))	D614G variant (Freuling et al. 2020), Antibody study by Wernike et al. (2020) used serology from lab infection with D614G variant (Freuling et al.	No	Unlikely: Luan et al., 2020b; Zhai et al., 2020	Possible

				2020)			
Masked palm civet	Paguma larvata		IP (S1/RBD): Trace/Low (Zhao et al. 2020); Pseudotyped entry: Low (Zhao et al. 2020); Binding Energy: Very low (Huang et al. 2020); Very low (Starr et al. 2022); Nil (Wu et al. 2020)		No	Low (Piplani et al.); Damas et al., 2020; Zhai et al., 2020; Likeley: Luan et al., 2020; Wu et al., 2020	Unlikeley
Chinese bamboo rat	Rhizomys sinensis	6			No	3 medium (Rhizomys pruinosus) (Karlssonlab 2022/Damas et al. 2020); (Spalax galili) Likely: Lam et al., 2020; (Spalax galili) Unlikeley Liu et al., 2020	Unkown
Red squirrel	Sciurus vulgaris		(Arctic ground squirrel) Binding Energy: High (Huang et al. 2020)		No	4 high (Karlssonlab 2022/Damas et al. 2020); unlikely Pach et al., 2020	Unkown
Wild boar	Sus scrofa	2	(Pig) Binding Energy: Medium/High (Wu et al. 2020)	(sus scrofa domesticus) No (Meekins et al. 2020; Vergara-Alert et al. 2021)	No	2 low (Karlssonlab 2022/Damas et al. 2020); Likely: Lam et al., 2020; Wu et al., 2020; Melin et al., 2020; Liu et al., 2020; Qiu et al., 2020	Unlikeley
Complex tooth flying squirrel	Trogopterus xanthipes		(Arctic ground squirrel) Binding Energy: High (Huang et al. 2020)		No		Unkown
Red fox	Vulpes vulpes		Binding Energy: Medium (Huang et al. 2020); High (Wu et al. 2020)	Yes (Porter et al. 2022); Tranmission borderline as maximal shedding (~4.9 log PFU/ml) less than minimal PFU (5.1 log PFU) used for innoculation (Porter et al. 2022)	No	2 low (Karlssonlab 2022/Damas et al. 2020); Likely: Luan et al., 2020; Liu et al., 2020; Lam et al., 2020; Praharaj et al., 2020	Possible
Cat	Felis catus		Binding Energy: Medium (Wu et al. 2020); High (Huang)		Yes		Possible
Dog	Canis familiaris		Binding Energy: Medium (Wu et al. 2020); High (Huang)		Yes		Possible
Human	Homo sapiens		IP (S1/RBD): Strong (Zhao et al. 2020); Pseudotyped entry: High (Zhao et al. 2020); High (Mykytyn et al. 2021); Binding	D614 and D614G	Yes	5 very high (Karlssonlab 2022/Damas et al. 2020); High (Piplani et al.)	Likely

			Energy: Very High (Huang et al. 2020); High (Wu et al. 2020)				

Supp. Table 2. HSM wild and domesticated animal SARS-CoV-2 susceptibility risk. Where a species has not been tested/predicted and a species from the same genus/family has been tested, these results are shown (with related species indicated in brackets), but may not reflect true susceptibility. Note in silico studies are predictions only and may not reflect true susceptibility. *Homo sapiens* shown for comparison. See Supp. data for spreadsheet version.

Species	HSM samples tested	HSM tested animals	HSM tested RT-OCR	Remarks
Rabbit/Hares	104	52	0	
Snake	80	40	0	
Stray cat	80	27	0	Including faeces
Hedgehog	67	16	0	
Chinese muntjac	18	6	0	
Dog	17	7	0	Including one stray dog
Badger	16	6	0	
Chinese bamboo rat	15	6	0	
Mouse	12	10	0	Captured around the market
Pig	6	NA	0	
Chicken	5	5	0	
Chinese giant salamander	5	3	0	
Crocodile	4	2	0	
Wild boar	4	2	0	
Soft-shelled turtle	3	2	0	
Fish	2	2	0	
Weasel	2	1	0	Captured around the market
Sheep	1	1	0	
Others	16	NA	0	
Total	457	188	0	

Supp. Table 3. Refrigerated and frozen animal samples at the HSM, warehouses supplying the HSM and animals caught and tested around the HSM tested for SARS-CoV-2 after Joint WHO-China Study (2021a) Table 4.

References

Babarleelephant, 2021. A tour into the Wuhan South China seafood market. http://babarlelephant.free-hoster.net/visiting-the-wuhan-seafood-market/

Boom FA, Brun PPHL, Bühringer S, Touw DJ. Microbiological monitoring during aseptic handling: Methods, limits and interpretation of results. Eur J Pharm Sci. 2020;155(August):105540. doi:10.1016/j.ejps.2020.105540

Cool K, Gaudreault NN, Morozov I, et al. Infection and transmission of ancestral SARS-CoV-2 and its alpha variant in pregnant white-tailed deer. Emerg Microbes Infect. 2022;11(1):95-112. doi:10.1080/22221751.2021.2012528

Damas J, Hughes GM, Keough KC, et al. Broad host range of SARS-CoV-2 predicted by comparative and structural analysis of ACE2 in vertebrates. Supp Info. Proc Natl Acad Sci U S A. 2020;117(36):22311-22322. doi:10.1073/pnas.2010146117

Epoch Times, 2020. The Secret of Wuhan Huanan Seafood Market Testing. 01 June 2020. https://www.epochtimes.com/gb/20/5/31/n12150755.htm. Archived at https://archive.ph/btWFY

Gao, G., W. Liu, G. Wong, J. Wang, F. Wang, and M. Li. 2022. "Surveillance of SARS-CoV-2 in the Environment and Animal Samples of the Huanan Seafood Market." *Research Square*.

Huang X, Zhang C, Pearce R, Omenn GS, Zhang Y. Identifying the Zoonotic Origin of SARS-CoV-2 by Modeling the Binding Affinity between the Spike Receptor-Binding Domain and Host ACE2. J Proteome Res. 2020;19(12):4844-4856. doi:10.1021/acs.jproteome.0c00717

Jemeršić L, Lojkić I, Krešić N, et al. Investigating the presence of sars cov-2 in free-living and captive animals. Pathogens. 2021;10(6). doi:10.3390/pathogens10060635

Joint WHO-China Study. 2021a. "WHO-Convened Global Study of Origins of SARS-CoV-2: China Part. Joint Report". https://www.who.int/publications-detail-redirect/who-convened-global-study-of-origins-of-SARS-CoV-2-china-part

Joint WHO-China Study. 2021b. "WHO-Convened Global Study of Origins of SARS-CoV-2: China Part. Joint Report - ANNEXES." https://www.who.int/docs/default-source/coronaviruse/who-convened-global-study-of-origins-of-sars-cov-2-china-part-annexes.pdf.

Karlssonlab. 2022. SARS-CoV-2 predicted binding scores for non-human species (including 116 new mammals). http://Karlssonlab.org/risk-scores/

Koopmans, 2022. Global Virus Network: Forefront of Virology COVID-19 Webinar Featuring Dr. Marion Koopmans. https://gvn.org/SARS-CoV-2-response-efforts/gvn-forefront-of-virology-covid-19-webinar-series-featuring-dr-marion-koopmans/, https://www.youtube.com/watch?v=3mDjV0Mmtx8&t=1146s

Lam SD, Bordin N, Waman VP, et al. SARS-CoV-2 spike protein predicted to form complexes with host receptor protein orthologues from a broad range of mammals. Sci Rep. 2020;10(1):1-14. doi:10.1038/s41598-020-71936-5

Liu Y, Hu G, Wang Y, et al. Functional and genetic analysis of viral receptor ACE2 orthologs reveals a broad potential host range of SARS-CoV-2. Proc Natl Acad Sci U S A. 2021;118(12):1-9. doi:10.1073/pnas.2025373118

Luan J, Lu Y, Jin X, Zhang L. Spike protein recognition of mammalian ACE2 predicts the host range and an optimized ACE2 for SARS-CoV-2 infection. Biochem Biophys Res Commun. 2020;526(1):165-169. doi:10.1016/j.bbrc.2020.03.047

Meekins DA, Morozov I, Trujillo JD, et al. Susceptibility of swine cells and domestic pigs to SARS-CoV-2. Emerg Microbes Infect. 2020;9(1):2278-2288. doi:10.1080/22221751.2020.1831405

Melin AD, Janiak MC, Arora PS, James P. Comparative ACE2 variation and primate COVID-19 risk 2. 2020. BoiXriv. doi: https://doi.org/10.1101/2020.04.09.034967

Moreira-Soto A, Walzer C, Czirják G, et al. Serological Evidence That SARS-CoV-2 Has Not Emerged

in Deer in Germany or Austria during the COVID-19 Pandemic. Microorganisms. 2022;10(4). doi:10.3390/microorganisms10040748
Mykytyn AZ, Lamers MM, Okba NMA, et al. Susceptibility of rabbits to SARS-CoV-2. Emerg Microbes Infect. 2021;10(1):1-7. doi:10.1080/22221751.2020.1868951
Pach S, Nguyen TN, Trimpert J, Kunec D, Osterrieder N, Wolber G. ACE2-Variants Indicate Potential SARS-CoV-2-Susceptibility in Animals: A Molecular Dynamics Study. Mol Inform. 2021;40(9):1-18. doi:10.1002/minf.202100031
Ohno et al. 2014 https://www.ncbi.nlm.nih.gov/pmc/articles/PMC3986730/#__ffn_sectitle
Piplani S, Singh PK, Winkler DA, Petrovsky N. In silico comparison of SARS-CoV-2 spike protein-ACE2 binding affinities across species and implications for virus origin. Sci Rep. 2021;11(1):1-12. doi:10.1038/s41598-021-92388-5
Praharaj MR, Garg P, Khan RIN, et al. Prediction analysis of SARS-COV-2 entry in Livestock and Wild animals. bioRxiv. Published online 2020:2020.05.08.084327.
Qiu Y, Zhao Y, Wang Q, et al. Predicting the angiotensin converting enzyme 2 (ACE2) utilizing capability as the receptor of SARS-CoV-2. Microbes Infect. 2020;22(4-5):221-225. doi:10.1016/j.micinf.2020.03.003
Quay S.C. 2021b. An Analysis of the Facts and Circumstances of the Worobey Science Perspective Paper Suggests it Makes No Contribution to the Investigation of the Origin of SARS-CoV-2. Zenodo. Published online 2021. doi:10.5281/zenodo.5717589
Romer labs, 2022. SurfACE™ Boot Cover Swabs. https://archive.ph/6NynU
Roy C, Mandal SM, Mondal SK, et al. Trends of mutation accumulation across global SARS-CoV-2 genomes: Implications for the evolution of the novel coronavirus. Genomics. 2020;112(6):5331-5342. doi:10.1016/j.ygeno.2020.11.003
Shi J, Wen Z, Zhong G, et al. Susceptibility of ferrets, cats, dogs, and other domesticated animals to SARS-coronavirus 2. Science (80-). 2020;368(6494):1016-1020. doi:10.1126/science.abb7015
Starr TN, Zepeda SK, Walls AC, et al. ACE2 binding is an ancestral and evolvable trait of sarbecoviruses. Nature. 2022;603(7903):913-918. doi:10.1038/s41586-022-04464-z
Stephanie M. Porter1, Airn E. Hartwig2, Helle Bielefeldt-Ohmann3, Angela M. Bosco- Lauth2* and JJR. Susceptibility of wild canids to severe acute respiratory syndrome coronavirus 2 (SARS-CoV-2). bioXriv. Published online 2022. doi:10.1101/2022.01.27.478082
Technical Safety Services, 2022. The importance of gloved fingertip sampling. https://archive.ph/kuDky
Vergara-Alert J, Rodon J, Carrillo J, et al. Pigs are not susceptible to SARS-CoV-2 infection but are a model for viral immunogenicity studies. Transbound Emerg Dis. 2021;68(4):1721-1725. doi:10.1111/tbed.13861
Wernike K, Aebischer A, Michelitsch A, et al. Multi-species ELISA for the detection of antibodies against SARS-CoV-2 in animals. Transbound Emerg Dis. 2021;68(4):1779-1785. doi:10.1111/tbed.13926
WHO Mission. 2021. 11-person team analyzing the origins of COVID-19 in Wuhan. Pre report release. https://docplayer.net/227382966-Who-mission-11-person-team-analyzing-the-origins-of-covid-19-in-wuhan-report-release-expected-10-14-days-from-now.html
Worobey, Michael, Joshua I. Levy, Lorena M. Malpica Serrano, Alexander Crits-Christoph, Jonathan E. Pekar, Stephen A. Goldstein, Angela L. Rasmussen, et al. 2022a. “The Huanan Market Was the Epicenter of SARS-CoV-2 Emergence.” *Zenodo*.
Worobey, Michael, Joshua I. Levy, Lorena Malpica Serrano, Alexander Crits-Christoph, Jonathan E. Pekar, Stephen A. Goldstein, Angela L. Rasmussen, et al. 2022b. “The Huanan Seafood Wholesale Market in Wuhan Was the Early Epicenter of the COVID-19 Pandemic.” *Science*, July, abp8715.
Wu L, Chen Q, Liu K, et al. Broad host range of SARS-CoV-2 and the molecular basis for SARS-CoV-2 binding to cat ACE2. Cell Discov. 2020;6(1). doi:10.1038/s41421-020-00210-9
Zhai X, Sun J, Yan Z, Zhang J, Zhao J, Zhao Z, Gao Q, He W-T, Veit M, Su S. Comparison of SARS-CoV-2 spike protein binding to human, pet, farm animals, and putative intermediate hosts ACE2 and

ACE2 receptors. bioXriv. Published online 2020. doi:10.1101/2020.05.08.084061
Zhao X, Chen D, Szabla R, et al. Broad and Differential Animal Angiotensin-Converting Enzyme 2 Receptor Usage by SARS-CoV-2. Gallagher T, ed. J Virol. 2020;94(18). doi:10.1128/JVI.00940-20